UNIVERSITY „POLITEHNICA" of BUCHAREST

DOCTORAL SCHOOL ETTI-B

SUMMARY OF PhD THESIS

Modern Methods for Control of Power Converters with Variable Reference Signals

Author: **Sergiu Oprea**

Committee

President	**Prof. Dr. Ing. Gheorghe Brezeanu**	from	**Univ. Politehnica Bucharest**
PhD Supervisor	**Prof. Dr. Ing. Constantin Rădoi**	from	**Univ. Politehnica Bucharest**
Referent	**Prof. Dr. Ing. Dan-Alexandru Stoichescu**	from	**Univ. Politehnica Bucharest**
Referent	**Prof. Dr. Ing. Alexandru Șerbanescu**	from	**Military Technical Academy, Bucharest**
Referent	**Prof. Dr. Ing. Gheorghe Gavriloaia**	from	**University of Pitești**

BUCHAREST 2018

Table of Content

1 Introduction

1.1 Domain of this PhD Thesis

The subject treated in this thesis belongs to the power electronics, namely the control of the static power converters operating with variable reference signals such as the inverters, the active power filters and the controlled rectifiers. The topic is topical given the importance of increasing energy efficiency globally. Also, the rapid development of energy conversion systems from alternative sources (solar panels, wind generators, etc.) gives rise to increased attention from the scientific community for finding new control methods for the power converters involved.

1.2 Purpose of this PhD Thesis

The present paper contributes to control methods for power converters operating with variable reference signals. Among the established control methods for this kind of power converters, the author deals in detail with resonant control considering that it provides maximum performance and flexibility and is recognized by the scientific community as the modern method of control in this case. Both the theoretical aspects of modeling the behavior of resonant controllers as well as the practical aspects related to the implementation of this type of control in the two fundamental domains, s and z are addressed. Aspects related to the practical implementation of resonant control are of great importance so that an important part of the thesis deals extensively with these aspects. It is proposed to deploy this type of control using low cost solutions to facilitate its deployment in low-cost applications such as residential ones. The proposed methods are validated by measurements made on the hardware platform implemented in practice using commonly available electronic components on the market.

1.3 Content of this PhD Thesis

Chapter 1 presents the scope and purpose of the PhD thesis as well as the content of the thesis chapters.

Chapter 2 presents converters that operate with variable reference signals as well as the control methods developed specifically for these converters. Also presented are the usual reference systems, systems used to analyze the converter as well as the associated control system. For each control method, the advantages and disadvantages as well as the reference system in which the controller operates are presented.

Chapter 3 deals with the implementation of the resonant controller in the two fundamental domains: the continuous time domain (*s*) and the discrete time domain (*z*). The author proposes a few circuit topologies that can be used to implement the *Proportional-Resonant* (*PR*) controller in the s-domain. For each circuit type there are presented the electrical diagram, the equations describing the operation as well as the *Bode* diagrams. The advantages and disadvantages of each type of circuit are also discussed. For z-domain implementation, specific topologies as well as adverse effects from various specific processes such as discretization and quantization are discussed. The effect of noise and finite resolution of the ADC converter on *PR* controller performance are also discussed in detail. The author presents in detail the effects of the finite gain of the resonant term on PR controller performance such as unit-step time response and stationary error. The author proposes a method of implementing the resonant term based on the phase-sensitive amplifier, a method that avoids the adverse effects introduced by the quantization process, and makes it possible to implement resonant control using fixed-point 16-bit processors whose cost is considerably lower than floating-point processors traditionally used to implement this type of control.

Chapter 4 discusses in detail the control of the three major categories of converters that operate with variable references using *PR* control. For each type of converter, a *PSIM* model has been developed and performance measured using various control methods. As original contributions, the author proposes to introduce a resonant term for controlling the low distortion rectifier based on the *Boost* converter as well as the use of hybrid control. This chapter also addresses the issue of assessing the stability of the control system. The usual analysis techniques for linear, invariant time systems such as *Nyquist* and *Bode* diagrams and sensitivity are presented.

Chapter 5 outlines the practical results obtained by the author as well as the hardware platforms used. Performance evaluation of control methods is performed using a low-power single-phase inverter and a control board that can be used to implement both the digital control and the hybrid control proposed in the previous chapter. The performances of the *PR* controller implemented in the s-domain are evaluated using frequency analysis (*Bode* diagrams) as well as time analysis. The practical results obtained are compared with those obtained from the simulations.

The annexes present the *PSIM* and *MATLAB* models used throughout this thesis. Also presented are the electrical diagrams of the hardware modules as well as the images during the tests performed using these modules.

2 The Control of Power Converters with Variable References

Control of static power converters working with time-varying reference signals like the power inverters and *Active Power Filters* (*APF*) is traditionally performed using "*Proportional-Integral*" (PI) controllers operating in *Synchronous Reference System* (ScRS). A series of coordinate transformations such as *Clarke* and *Park* transformations are required to ensure the operation of the *PI* controller in the synchronous reference system. This eliminates the main disadvantage associated with the *PI* controller, namely the impossibility of eliminating stationary error if the reference and error signals vary over time. A block diagram of such implementation is shown in Fig. 2.1.

The high complexity of such a solution makes it difficult to model and implement the control system. The final cost of the solution is also high because it requires the use of signal processors with high computing power.

A wide range of control methods dedicated to this type of power converters has been proposed by researchers in the field over time. The main objective in mind was achieving results similar to those achieved by *PI* control for DC-DC converters namely zero stationary error, simplicity of implementation and a simple theoretical analysis.

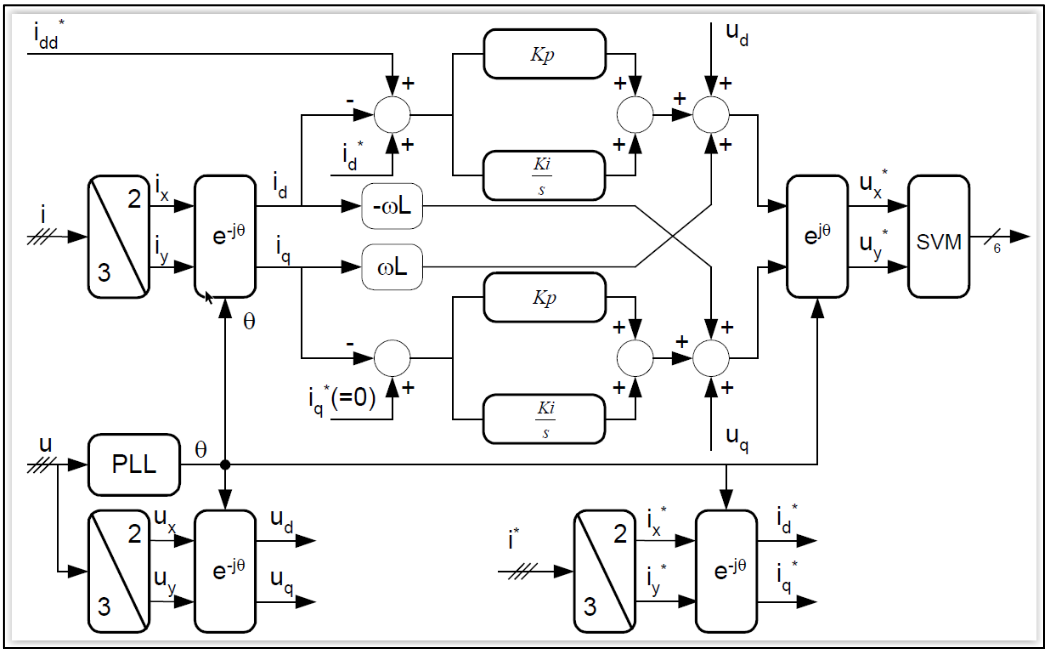

Fig. 2.1 Three-phase inverter controlled using PI-dq controllers [1]

2.1 Power Converters with Variable Reference Signals

The first category of power converters operating with time-varying reference signals are inverters. In Fig. 2.2 (a) shows a single-phase inverter currently in use in *UPS* applications. Both the (i_L) and the output voltage (u_L) can be controlled and the associated reference signals are sinusoidal or include harmonic components. In Fig. 2.2 (b) presents a three-phase inverter with balanced load. It is possible to control the three line currents i_A, i_B and i_C in the case of electric machines or the voltage u_A, u_B and u_C in case of "voltage source" inverters.

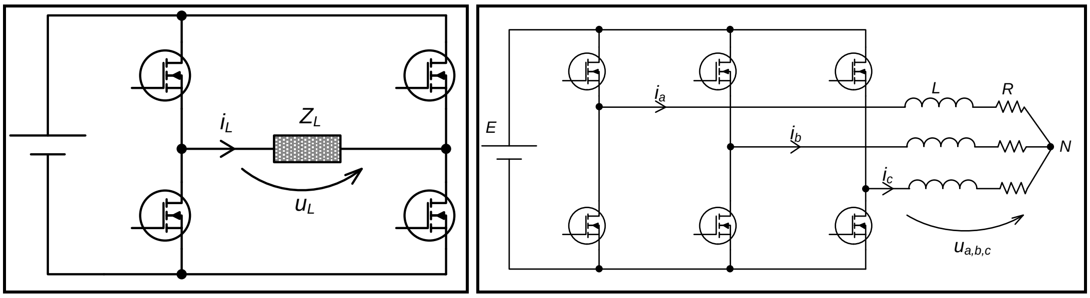

(a) *(b)*

Fig. 2.2 Single-phase inverter and three-phase inverter with balanced load

Active Power Filters (*APFs*) are circuits capable of improving the power factor for nonlinear loads by eliminating line current harmonics. *APFs* generally offer improved performance compared to passive filters, but at a higher cost. The electrical diagram of a parallel type *AFP* is shown in Fig. 2.3 (a). In this case the inverter supplies to the load only the harmonic components of the absorbed current so that the generator provides only the fundamental component of the current which is sinusoidal.

The controlled rectifiers are the third major category of converters where the reference signals are variable. The power range of this type of converter is very wide from a few watts in the case of LED lighting applications up to many MW in the case of industrial applications (electrolysis baths, rolling mills, etc.). In this type of converter, the control strategy focuses on two desiderata: controlling the magnitude of the output parameter (voltage in most cases) as well as controlling the shape of the input current. The shape of the input current is very important for maintaining a high power factor. In Fig. 2.3 (b) shows the electrical diagram of a *Vienna* rectifier. This type of three-phase rectifier is found in the industry at high power, where it is necessary to control the magnitude of the continuous output voltage as well as to maintain a high power factor.

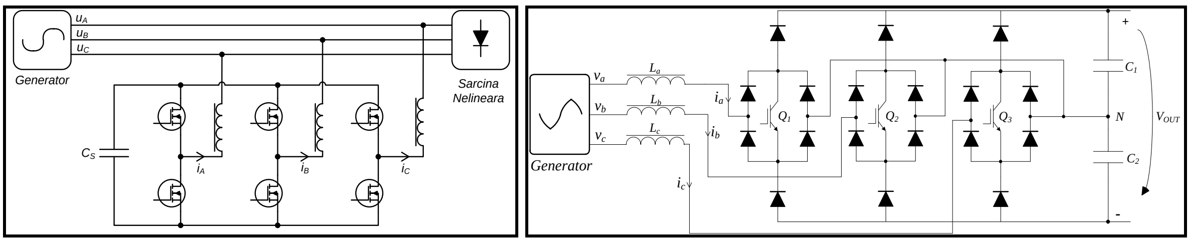

(a) *(b)*

Fig. 2.3 Active Power Parallel Filter (a) and Vienna Rectifier (b)

2.2 Types of Controllers

2.2.1 The Hysteretic-type Controller

This type of controller was first proposed for inverter control and AFPs in the *Stationary Reference System* (StRS). For many years, it has been the only type of control that provides high performance for variable time reference signals [2, 3]. Hysteretic control is used to control inverters [6], *APFs* as well as *PFC* circuits. Figure 2.4 (a) presents such a load-current controller for a single-phase inverter. By extension, the same configuration is also used for three-phase inverters to control line current in the three phases.

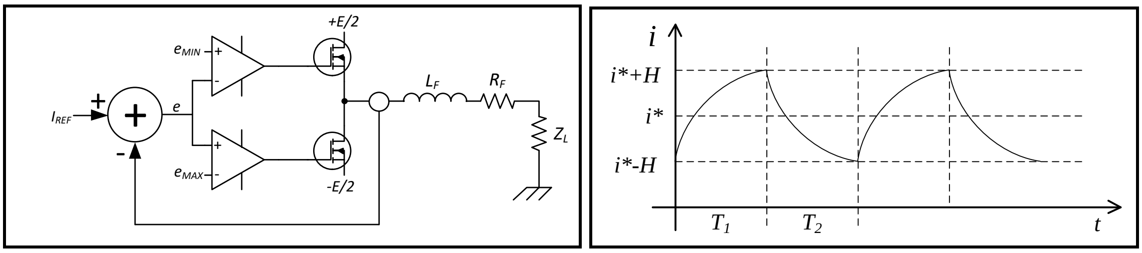

(a) (b)

Fig. 2.4 Hysteresis type controller (a) and current evolution over time (b) [7]

The control signal for the power switches is obtained by comparing the error signal e with the two e_{MIN} and e_{MAX} thresholds. If e is less than e_{MIN}, then the higher switch to increase the current is operated in the "closed" state. Similarly, if e is greater than e_{MAX}, then the lower switch is operated in the "closed" state causing the output current to decrease. In a real implementation, an additional control circuit of the switches ensures their protection as well as the insertion of a "*dead time*" between the switching states of the two switches.

This type of controller, which belongs to the nonlinear control family, comes with a number of notable advantages: it is simple to implement and is unconditionally stable [33], ensures good accuracy and excellent response to variations in the reference or feedback signal [2, 4] and has a reduced sensitivity to variation of load parameters [5].

Although this type of controller has been widely used for controlling currents in inverters and AFPs, there are a number of associated disadvantages:

- The switching frequency is variable. This makes it difficult to design additional filters to eliminate *EMI*. Also, the variable frequency may affect the operation of the power elements. Because of the variable switching frequency, the parasitic resonances of the output filter or the electric machine constituting the load can be excited [5].
- Selective elimination of harmonics in *APFs* is virtually impossible with this type of controller.
- For three-phase systems, this controller is sensitive to interference between the three phases. Analytical solutions have been proposed for this problem, but they are sensitive to system parameters estimation.

Another drawback is related to the complexity of the analysis in assessing the stability of the control system. Being a nonlinear controller, analytical techniques are complicated and sometimes only approximate, making it impossible to find an analytical solution to the problem [34].

2.2.2 Sliding Mode Controller

Switching power converters are nonlinear systems with a time-varying structure. Based on this observation, control with sliding variables known in the literature as "*Sliding Mode Control*" [7] can be introduced. This type of control is used successfully for the control of inverters, *APFs* and *PFC* circuits as well as for the implementation of various state observers used for control of electrical machines.

Intuitively, it is noticeable that a linear and time-invariant system (described by first-order differential equations) is much easier to control than a nonlinear and time-varying system. Starting from this observation, the control strategy in the case of sliding-mode control focuses on finding a linear system of the order one whose dynamics is equivalent to the dynamics of the original non-linear system [29]. At this point, the original problem of control of the nonlinear system of the *n* order is reduced to control of the linear system of the first order. "The main advantages of sliding control are the simplicity of implementation, stability, adaptability to large variations of system parameters and direct command of the power switches" [7].

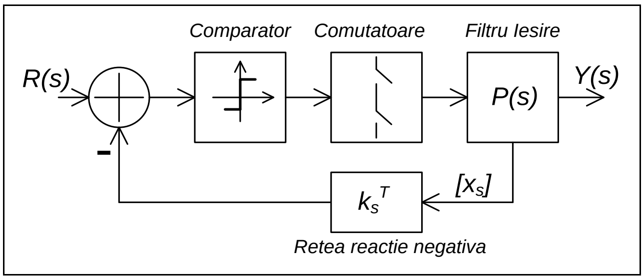

Fig. 2.5 A non-linear system with variable structure [7]

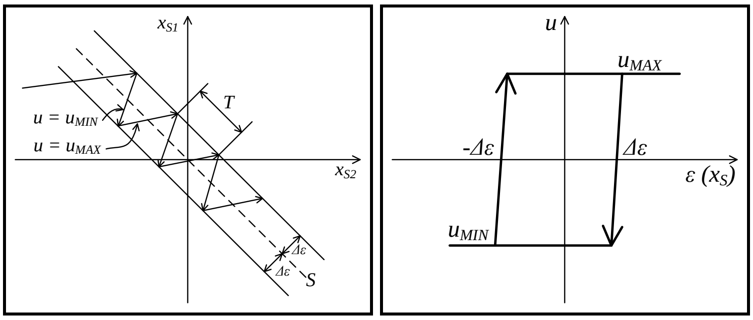

Fig.2.6 Sliding trajectory and the evolution of control signal u as a function of error [7]

If a bounded region of $\pm\Delta e$ near the S is considered, the state variables will evolve within this region, basically "sliding" on the S-trajectory. In the specific case of a system similar to that in Fig.2.5, state variables are controlled directly by the state of the two switches. The value of the hysteresis depends on the frequency with which the two switches switch; a null hysteresis value implies an infinite switching frequency.

The simplest form of implementation of this type of controller is based on a hysteresis comparator similar to Fig. 2.4 (a). The switching frequency is variable, which is one of the drawbacks of this implementation. Removing this disadvantage has been one of the major research goals for many years. A number of changes have been proposed, among which the introduction of auxiliary signals for generating commutation commands and a fixed frequency PWM signal generation scheme, where the modulator signal is provided by the sliding-mode controller [7].

2.2.3 The „*Deadbeat*" Controller

This type of controller is part of the predictive control family and can only be implemented in the discrete (digital) time domain [28]. Its popularity has increased significantly with the widespread introduction of digital control [8, 28]. The main idea behind this type of control comes from the analysis of the closed-loop transfer function of a discrete system:

$$H_S(z) = \frac{H_C(z)H_P(z)}{1+H_C(z)H_P(z)} \tag{2.1}$$

Where $H_S(z)$ is the control-output transfer function, $H_C(z)$ is the transfer function of the controller and $H_P(z)$ is the transfer function of the controlled system, i.e. the transfer function of the power converter, in this case.

If a minimum delay is required for all working frequencies, we can note $H_S(z) = z^{-2}$. The two-cycle delay is associated with the calculations required to implement the controller (first cycle) and the PWM modulator, the output filter, and possibly the inverter dead time (second cycle) [8].

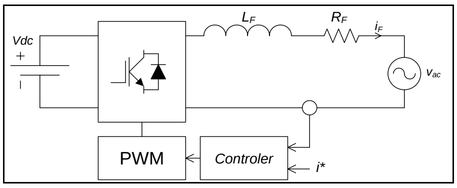

Fig. 2.7 The output filter of an inverter

If it is considered an inverter whose output is connected to a filter composed of L_F inductance and R_F resistor (Fig.2.7), the *Zero-Order-Hold (ZOH)* approximation can be used for the discretizing of the associated transfer function:

$$H_F(s) = \frac{1}{sL_F+R_S} \tag{2.2}$$

It is considered the transfer function of the converter in the discrete time domain obtained by discretizing the original function with ZOH:

$$H_P(z) = z^{-1}Z\left\{\mathcal{L}^{-1}\left[\frac{1-e^{-sT_S}}{s}H_L(s)\right]\right\} = \frac{z^{-2}}{R_F}\frac{1-e^{-\tau}}{1-z^{-1}e^{-\tau}} \tag{2.3}$$

Where $\tau = R_F T_S / L_F$

Using (2.1) and (2.3), the transfer function of the „*Deadbeat*" controller becomes:

$$H_{DB}(z) = \frac{R_F}{1-e^{-\tau}}\frac{1-z^{-1}e^{-\tau}}{1-z^{-2}} \tag{2.4}$$

This type of controller provides very good performance but cannot reduce stationary error to zero because of the two delay cycles. Also, to ensure maximum performance, it is necessary to accurately estimate the parameters of the controlled system.

2.2.4 The *PI Controller* in Synchronous Reference System

The "*Proportional-Integral*" controller (*PI*) is the most popular type of controller and one of the most extensively studied and used [29]. The frequency response of the *PI* controller has a native origin pole and a zero whose position can be controlled. The *PI* controller is widely used to control *DC-DC* converters, especially those using "*Programmed Current Mode Control*" as a control strategy [35]. The *PI* controller has infinite gain at zero frequency, being able to eliminate the stationary error in the case of *DC* signals or with very slow variation over time. For signals with a non-zero frequency, this controller cannot provide the elimination of stationary error, its performance in this case being modest.

Solving the problem of low gain for alternate signals is done by using coordinate transformations. In the case of three-phase systems, the *Park* transformation (Figure 2.8) is used. The two *PI* controllers are used for *id* and *iq* control, these two signals being *DC* now [9]. This eliminates stationary errors, but the complexity of the control system increases considerably.

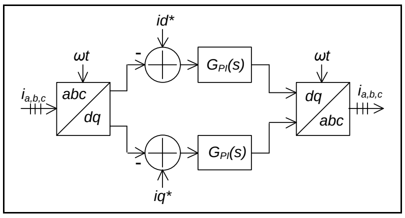

Fig. 2.8 PI controller in ScRS (balanced three-phase system)

In the case of *AFPs*, the selective elimination of harmonics is sometimes required. In this case, the angular velocity ω_0 associated with the *Park* transformation must be set accordingly to the harmonics to be eliminated; $\omega_0 = h\omega_1$ where *h* is the rank of the harmonics to be eliminated and ω_1 the angular frequency of the fundamental. For each controller associated with a harmonic component, the K_P and K_I parameters must be individually adjusted [10].

$$G_{PIn}(s) = K_{Pn} + K_{In}\frac{1}{s} \tag{2.5}$$

A typical inverter application connected to the national network and controlled using *PI* controllers in ScRS is shown in Fig. 2.9. The complexity is very high and a high-power *DSP* is required for implementation. For unbalanced systems, two *PI* controllers are used for each sequence. In this case, the complexity is very high, requiring a double number of controllers and a double set of coordinate transformations.

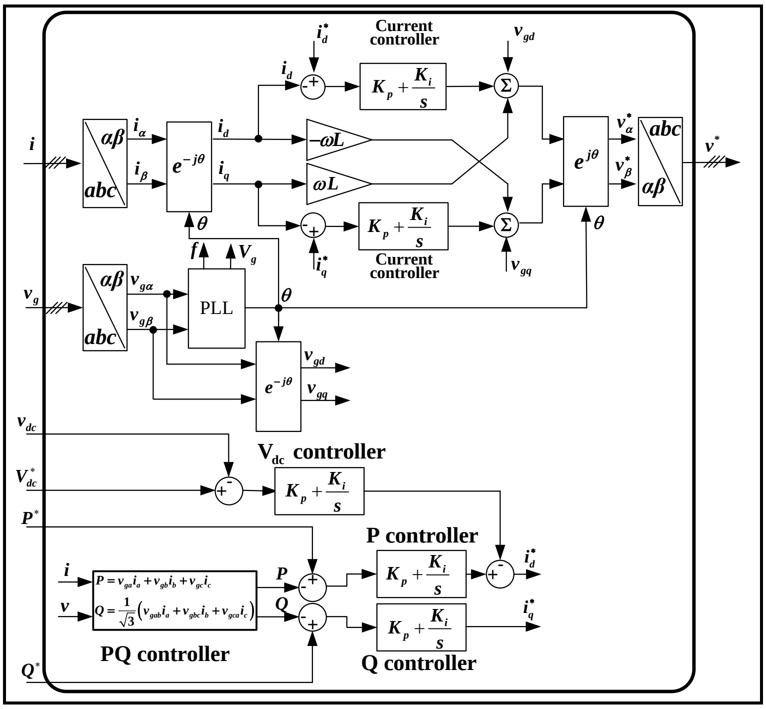

Fig. 2.9 Typical application for controlling an inverter connected to the national network

2.2.5 The Repetitive Controller

This type of controller has been proposed in an attempt to minimize stationary errors for converters that work with harmonic reference signals such as *AFPs*. The basis of this type of controller is the principle of the internal model: zero stationary errors can be obtained for a given reference if the model of the reference generator is included in the controller model [11].

Repetitive control was originally proposed for *SISO*, linear and invariant systems over time. The originality of this type of control lies in the development of an internal model for any periodic signal generator with a known period T. The model is of the form:

$$M_{IC}(s) = \frac{1}{1-e^{-Ts}} \tag{2.6}$$

If the control loop includes the $M_{IC}(s)$, then the system is able to track a periodic reference with the T period, with a stationary zero error. A typical implementation in the continuous time domain is represented in Fig. 2.10.

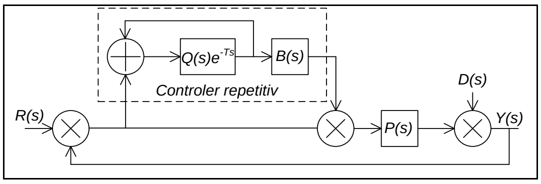

Fig. 2.10 S-domain repetitive controller

The term $M_{IC}(s)$ has no limitations on gain at high frequencies, theoretically there are no restrictions even at infinite frequency values. This is undesirable in the case of practical implementation, especially in the case of power converters. Changes have been proposed, such as inserting a low-pass filter into the loop to limit gain at high frequencies. This increases immunity to noise and robustness of the solution but reduces performance at high frequencies.

Frequency response has an infinite array of poles on the axle, placed equidistant from each other. Placed in a closed-loop control system, this controller provides infinite gain at the *1/ndTs* frequencies resulting in zero stationary errors for these frequencies. In the case of a fundamental frequency signal *f1* and the associated harmonics, the condition to be satisfied is $n_d T_s = 1/f_1$.

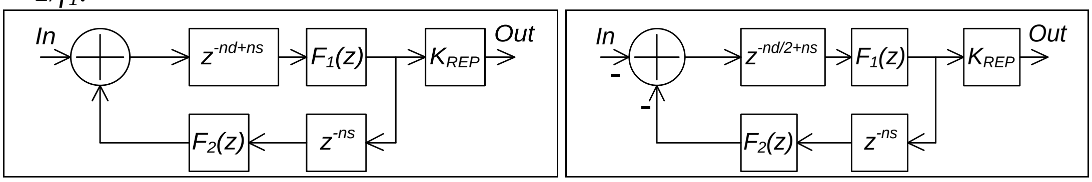

Fig. 2.11 Repetitive controller that operates with odd/even harmonics, and only odd harmonics

However, there are a number of drawbacks that need to be considered if this type of controller is to be used:

- n_s is an integer. This limits the options in terms of the frequency of the frequencies where the gain peaks occur.
- n_s must be the same for all frequencies associated with harmonics. If the frequency response of the converter output filter is not proportional to frequency, such as *LCL* filters, then the controller is unable to compensate for the phase errors input by this filter. This is a serious limitation that can negatively affect the stability of the controlled system.

2.2.6 The *Proportional-Resonant* Controller

"*Proportional-Resonant*" type controllers have been introduced as a control alternative for inverters [15], *APFs* [12], controlled rectifiers [13], *STATCOM*, *DVR* [18] and motor control systems [19]. This type of controller eliminates stationary error for variable references while being able to operate directly in *StRS*. It is one of the most studied controllers due to its flexibility, performance and simplicity [12-19]. Fig. 2.12 presents a specific implementation of a three-phase inverter using *PR* controllers in *StRS* [16].

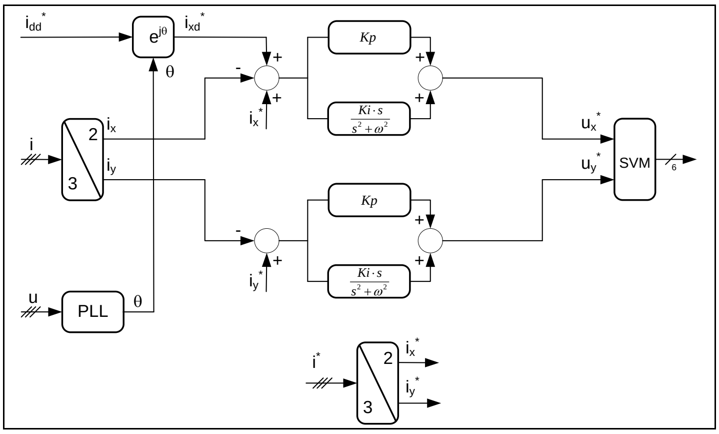

Fig. 2.12 Three-phase inverter controlled by PR controllers in StRS

It is noticeable that the implementation based on PR-type controllers is significantly less complex than the classical *PI*-based implementation. The *PR* controller acts on both sequences (positive and negative) for unbalanced systems; so the complexity of the control system is greatly reduced, and it is not necessary to explicitly extract the symmetric sequences.

The general form in the *Laplace* domain of a *PR* controller is:

$$G_C(s) = K_P + K_R \frac{s}{s^2 + \omega_R^2} \tag{2.11}$$

where K_P - the gain of the proportional term, K_R - the gain of the resonant term, ω_R - the resonance frequency

Additional resonant terms can be added if the application asks for it (such as the selective elimination of harmonics for *APFs*). The gain of the resonance frequency is infinite, similar to a second-order system where the damping factor is zero. Such a controller cannot be implemented using analog or digital circuits because it is impossible to obtain an infinite gain in practice. The practical form of a *PR* controller is:

$$G_C(s) = K_P + K_R \frac{s}{s^2 + \xi s + \omega_R^2} \tag{2.12}$$

Where: ξ – damping ratio.

The second term of equation (2.11) is associated with a generalized integrator. Virtually a "sinus" signal will be integrated over time without introducing an additional phase error [17]. The existence of this term leads to a similarity between the *PI* type and *PR* type controllers, with the specification that in the case of the *PR* type, the integral term acts only on the signals with frequencies very close to the resonance frequency. The *PR* controller provides a high gain around its own resonance frequency, being able to eliminate the stationary error for variable time references.

2.2.7 Conclusions

A wide range of methods and improvements have been proposed for controlling converters operating with variable reference signals. Each method has associated advantages and disadvantages that can be used to control a particular type of converter.

Hysteretic control provides excellent performance in reference signal tracking and response to load variation. The major disadvantages of this controller are the variable switching frequency and the sensitivity to the variation of the converter parameters. Another disadvantage is related to the complexity of stability analysis methods. This type of controller requires analysis using non-linear control methods, which are generally difficult to apply.

Sliding mode control also provides excellent performance for variation of reference signal and load, but requires variable switching frequency. The proposed methods to ensure a fixed switching frequency adversely affect the performance of this type of control. Stability analysis methods are complex because this controller is a non-linear one.

The "*Deadbeat*" controller can only be implemented in the z-domain and belongs to the predictive control family. The performances obtained with this type of control are good, but depend to a great extent on the accuracy with which the parameters of the controlled system are estimated. The variation of these parameters adversely affects the "*Deadbeat*" controller.

The PI-type controller running in ScRS is widely used for controlling converters with variable reference signals, being the most popular and studied type of control. It provides excellent performance in eliminating the stationary error, but the control system has a very high complexity due to multiple changes of the reference system.

The repetitive controller was the first solution introduced for systems where the reference is time-varying and has harmonic components. This solution, although providing good performance, presents implementation difficulties. The required delay line is easy to implement in the z-field but difficult in the s-domain. There are also constraints on the frequency spectrum for the controlled signal.

The *PR* controller, implemented using the generalized integrator, has generated a special interest for the scientific community due to the flexibility it offers. This type of controller operates in *StRS* providing the same performance as the *PI* controller in *ScRS* but with a much lower complexity of the control system. It is the modern method of control adopted on a large scale for the control of converters with variable references.

The next chapter analyzes the implementation of the *PR* controller in the two fundamental domains: the continuous time domain (s) and the discrete time domain (z).

3 The Implementation of PR Controller in s and z domains

3.1. The Implementation of PR Controller in s-domain

In the literature, the presentation and analysis of the PR controller is in a high proportion in the s domain. However, when it comes to the practical implementation of this type of control it is in most cases in the z-domain. The main reason is the flexibility that digital implementation offers and the rapid development of solutions dedicated to this type of control. Implementation in the field has several advantages that can simplify the design process of this type of control. These can be listed:

- The maturity of the analysis methods in the s domain. The entire design process can be done in the s-domain and then it can be traversed in the z-domain by a number of well-known methods (Euler direct and inverse transformations, Tustin transformation, etc.)
- Implementation using active circuits such as operational amplifiers. This can result in substantial price reductions for some applications.
- Lack of constraints associated with discrete systems regarding the frequency spectrum of the signals. For discrete systems, the maximum frequency must comply with the Nyquist criterion; in the case of analogue systems, this is not necessary.
- A large number of simulators operate in the continuous time domain. Here are SPICE-based ones.

The main drawback of implementation in the s-domain is the lack of flexibility. An example of this can be the PR controllers operating with variable frequencies. In this case, the adjustment of the central frequency for analogue systems is extremely difficult and impractical. In the case of digital systems, this is done easily by modifying the coefficients associated with the filter.

In Fig. 3.1 shows a possible configuration of a *PR* controller in the s-domain. The implementation is based on an operational amplifier and passive components of type R, L and C. The presence of the *LC* series circuit in the amplifier's feedback loop modulates its gain according to the frequency. The impedance of the *LC* series resonant circuit is minimal at the resonance frequency, the gain being the maximum at this frequency. The resonance frequency is given by:

$$f_c = \frac{1}{2\pi\sqrt{LC}} \tag{3.1}$$

The circuit transfer function is:

$$\frac{V_{OUT}}{V_{FB}} = -\left[\frac{R_2}{R_1} + \frac{R_3}{R_1}\left(1 + \frac{sR_2C}{1+s^2LC}\right)\right] \tag{3.2}$$

Suppose $R_2 << R_1$ and $R_2 << R_3$:

$$\frac{V_{OUT}}{V_{FB}} \cong -\left[\frac{R_3}{R_1}\left(1 + \frac{sR_2C}{1+s^2LC}\right)\right] \tag{3.3}$$

The gain of the amplifier for frequencies different from the resonance frequency f_c is given by R_1, R_2 and R_4.

$$G_P \cong -\frac{R_3}{R_1} \tag{3.4}$$

This gain is associated with the proportional term and is frequency independent.

The scheme in Fig. 3.1 can be easily modified to support multiple resonance frequencies by adding additional resonant terms. In Fig. 3.2 is a diagram of a PR controller with three resonant frequencies: 50 Hz (fundamental frequency), 150 Hz (third harmonic) and 250 Hz (fifth harmonic).

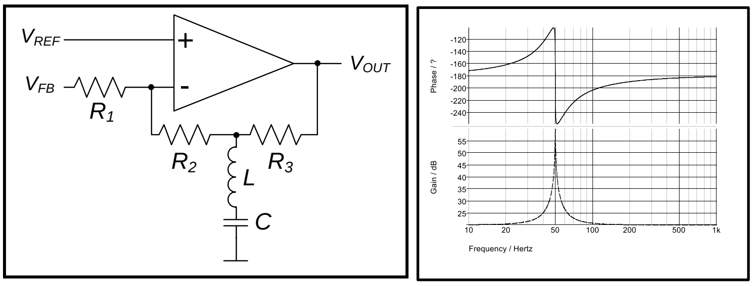

Fig. 3.1 PR controller implemented using LC circuit and the Bode diagrams (fr=50Hz)

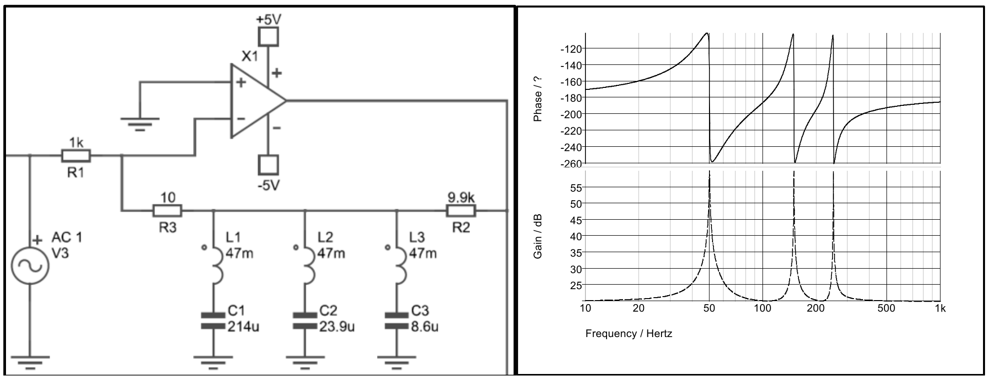

Fig. 3.2 Multiple resonant frequencies PR controller and the Bode diagrams

The topologies presented are simple and can be used successfully in inverter simulations, APFs and power factor correction circuits in the s-domain. There is, however, a major disadvantage associated with these circuits, namely the non-practical values for the *LC* circuit components. An inductor with a value of 47mH, good tolerance and high quality factor is very difficult to be produced in practice. The cost and dimensions of such a component are very high. Also, the capacitor is large and non-polarized. It must have a tight tolerance to avoid important errors that may affect the resonance frequency. Such a component has a very high price and occurs in series of values, finding the value required for the resonance frequency adjustment (generally different from the standard values), being virtually impossible. Under these circumstances, it is necessary to seek solutions that can be easily implemented using common components produced in large series at a low cost. Large components and wide tolerances such as inductors are also to be avoided.

Using the same principle of introducing into the loop of networks whose impedance varies with frequency topologies that can be used for *PR* controllers can be obtained. The "*double T*" type network, commonly used in the synthesis of "*band-stop*" filters, presents a specific response to a second-order system with a sharp decrease in gain at resonant frequency. The resonance frequency for such a network is given by:

$$f_C = \frac{1}{2\pi R_3 C_1} \tag{3.5}$$

The network's transfer function is:

$$H_T(s) = \frac{\omega_0^2 - \omega^2}{\omega_0^2 - \omega^2 - s\Delta\omega} \tag{3.6}$$

Where $\omega_0 = 1/RC$. The quality factor Q is 0.25.

In Fig. 3.3 is a possible configuration of a *PR* controller implemented using a "double T" type network introduced into the feedback loop of an inversion amplifier. The X3 repeater amplifier provides high input impedance for the "double T" network. Proportional gain is well defined for frequencies different from the resonance frequency and is given by:

$$G_P = -\frac{R_9}{R_1} \tag{3.7}$$

The quality factor is relatively small, as can be seen from the associated Bode diagrams.

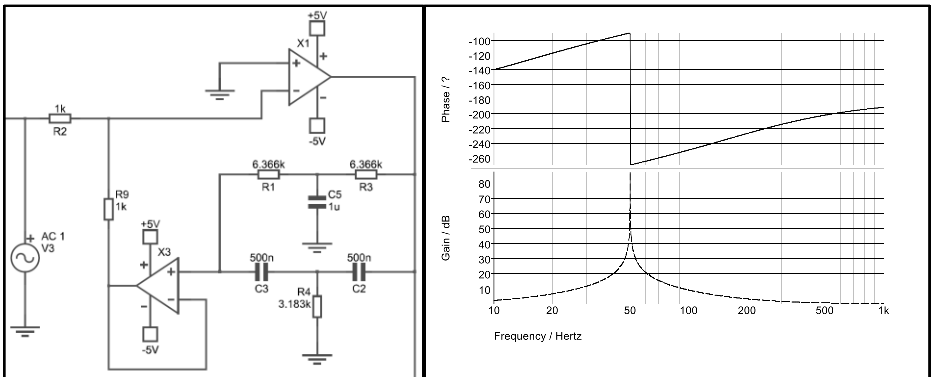

Fig. 3.3 PR controller implemented using a "double T" network

3.1.1. Conclusions

Implementation of *PR* controllers in the s-domain can be done using several amplifier topologies in which the feedback loop has introduced impedance elements that vary with frequency. The practical importance of these circuits is relatively limited due to their high sensitivity to component tolerances and very low flexibility. Basically, the resonance frequency cannot be dynamically adjusted, constituting a major disadvantage for applications requiring continuous control over this parameter, such as inverters connected to the national power distribution network or APFs.

S-domain implementation is, however, of interest when targeting applications where final cost is to be kept under control such as fixed frequency inverters that are part of "*Uninterruptible Power Supply*" (*UPS*) type systems.

The topologies presented may also be useful for simulating power circuits using simulators in the continuous time domain like SPICE. In this case, the influence of parasitic elements and noise on controller performance can be estimated using real components instead of the ideal ones commonly encountered in simulations.

3.2. Implementation of PR Controller in the z-domain

The implementation of this controller in the discrete domain is particularly important due to the fulminant development of the solutions dedicated to digital control. The digital implementation of controllers eliminates the disadvantages associated with analog implementations such as lack of flexibility, variation of parameters with component tolerance, and undesirable effects from aging components [28, 30]. The specialized literature presents the PR controller in the domain of s, one of the reasons being the maturity of the analysis made in this field. However, the vast majority of applications including PR controllers are implemented in the z-domain using microprocessors, digital controllers or *FPGAs*. For z-domain implementation, some discretization methods have been proposed, each with its own advantages and disadvantages. The effects of the discretization process cannot be neglected and the conclusions of the analysis in the field can be affected to a significant extent by these effects.

3.2.1. The Effects of the Discretization Process

The design of resonant controllers is generally done in the s domain. Stability of the control system is also evaluated in the s-domain, and then the entire controller is discretized using one of the dedicated methods discussed above and implemented in a *DSP*. The effects introduced by the quantization process as well as the implications for the actual implementation of the controller in the *DSP* should be carefully assessed to achieve the expected performance.

One of the adverse effects of the discretization process is the movement of poles and zeros [20]. Their original position in the complex plane s is different from their position in the z plane. The consequence of this frequency shift is the significant degradation of controller performance.

Fig.3.4 presents the *Bode* diagrams for the original resonant term in s and for the resonant term discretized with the Tustin method. The resonant term has a resonance frequency equal to 350 Hz. One can observe the same phenomenon that also appears in the discretization of the resonant term implemented with two simple integrators. The resonance frequency after the discretization process is 348.6 Hz; an error of about -1.4 Hz. The gain is significantly affected, basically being very low for the original 350 Hz.

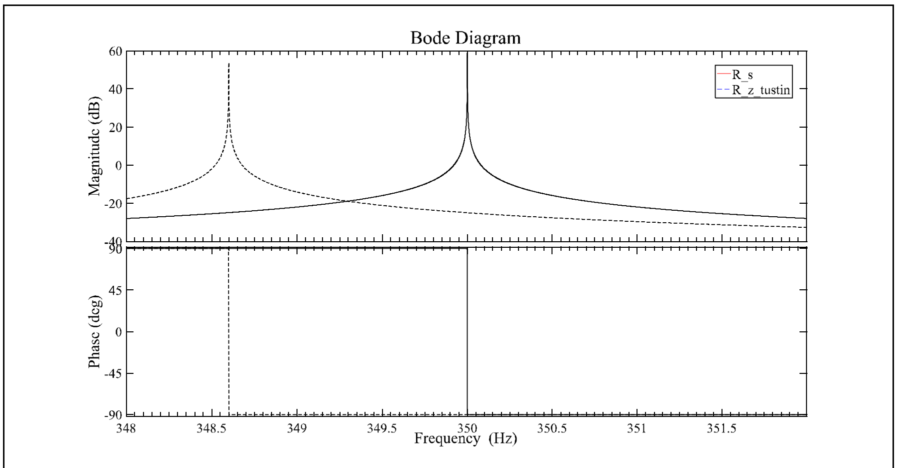

Fig. 3.4 Bode diagrams for Tustin discretization

3.2.2. The Effects of the Quantization Process

The implementation of the controller in the *DSP* involves the representation of the coefficients and the signal from the output of the analog-to-digital converter in a format supported by the *DSP*. This process introduces additional adverse effects to be taken into account for a good assessment of the performance of the controller. Most digital signal controllers use fixed-point representation on a fixed bit number that varies between 16 and 32 bits.

One of the side effects introduced by the coefficient quantization process is the shift of the polar frequency of a digital filter. It is possible to determine the variation of the position of poles p_i to the coefficients variation a_k by introducing the sensitivity function:

$$\frac{\partial p_i}{\partial a_i} = \left.\frac{z^{-k}}{-(z^{-1}\prod_{j=j\neq i,1}^{N}(1-p_j z^{-1}))}\right|_{z=p_i} \tag{3.8}$$

It can be noted that if the poles have close positions, the sensitivity to the disruption of the coefficients is high. In the case of the resonant term of the *PR* controller, the poles are complex conjugated having the same angular frequency. In this case, the associated sensitivity is extremely high. In [22] is proposed the following expression for moving the double pole frequency in the case of a system of the order M:

$$\Delta z_{pn} \approx \left[\frac{\sum_{k=1}^{N} -\Delta a_k z_{pn}^k}{\prod_{l=1,z_{pl}\neq z_{pn}}^{N}(z_{pn}-z_{pl})}\right]^{1/M} \tag{3.9}$$

For the resonant term, the effects of quantization can be extremely pronounced. For 16-bit quantization, the double pole frequency error is about 0.04 Hz. Gain is strongly affected by this error (Figure 3.5). When using the 24-bit and 32-bit quantization, the input error is small, basically the Bode plots for overlapping gain.

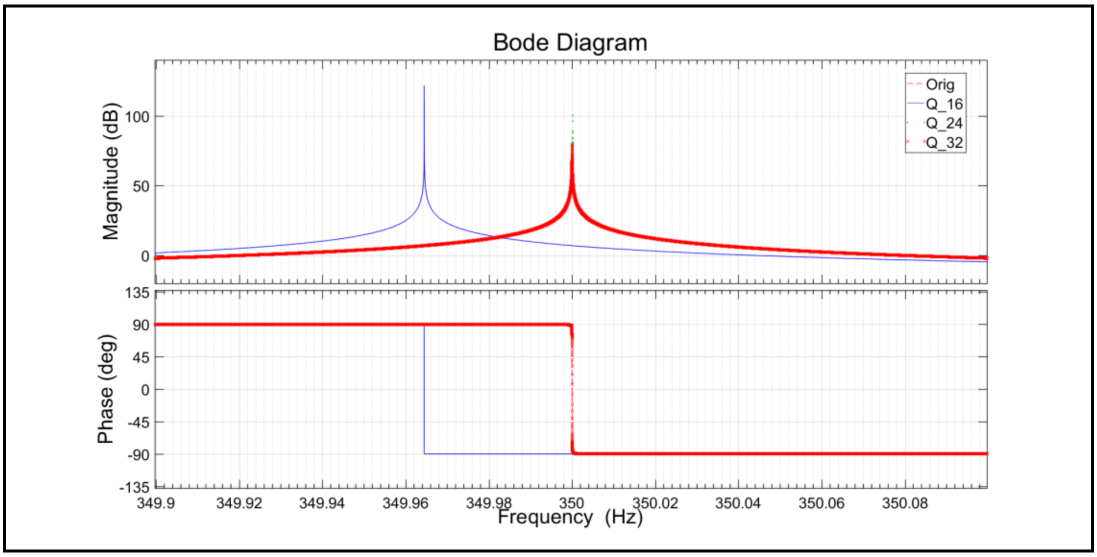

Fig.3.5 Bode plots for the original resonant term and 16, 24, and 32-bit quantized terms.

3.2.3. The Implementation Based on the Phase-sensitive Amplifier

The analysis of the effects introduced by the quantization process in the previous subchapter reveals virtually the impossibility of implementing the resonant term using a low cost DSP with 16-bit resolution and fixed-point representation. This is a major disadvantage if a low cost and low cost digital converter is to be designed. In view of this, the author proposes an implementation based on the phase amplifier principle known in the literature as "Lock-in Amplifier". The block diagram of such an amplifier is shown in Fig. 3.6.

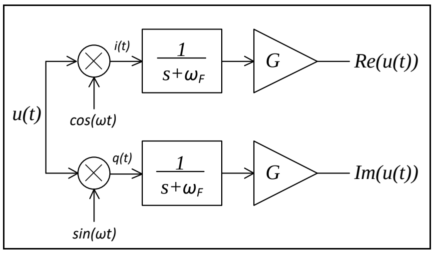

Fig. 3.6 Phase-sensitive Amplifier

The two *i(t)* and *q(t)* signals at the output of the multipliers are also called "*in phase*" or "*quadrature*" respectively. The associated expressions are:

$$i(t) = u(t)\cos(\omega t) \tag{3.10}$$

$$q(t) = u(t)\sin(\omega t)$$

If *u(t)* is:

$$u(t) = A_u\cos(\omega t)$$

Then:

$$i(t) = A_u\cos(\omega t)\cos(\omega t) = \frac{A_u}{2}[\cos(0) + \cos(2\omega t)] = \frac{A_u}{2}[1 - 2\sin^2(\omega t)] \tag{3.11}$$

$$q(t) = A_u\cos(\omega t)\sin(\omega t) = \frac{A_u}{2}[\sin(2\omega t) - \sin(0)] = \frac{A_u}{2}\sin(2\omega t) \tag{3.12}$$

The alternate components are filtered with a low-pass filter and the resulting DC component is amplified by the G amplifier. For different frequencies the DC component is null, virtually the output of the G amplifiers being null. The circuit behaves like an extremely narrow bandwidth filter with a central frequency equal to $\omega/2\pi$. If the low-pass filters are replaced by ideal multiplier outputs and the output of these integrators is multiplied by *sin(ωt)* or *cos(ωt)* reference signals, the resulting circuit behaves as a generalized integrator with the central frequency ω / 2π; the gain is infinite for the signals with the frequency $\omega/2\pi$ and the null for the signals having another frequency.

The resonant term implemented with the aid of the phase-sensitive amplifier principle has the block diagram represented in Fig. 3.7 (a). Generally, the *sin(ωt)* and *cos(ωt)* reference signals are available inside the control system being generated locally using controlled oscillators or PLL circuits.

For a PR controller, the resonance central frequency is known to be an initial design parameter. Considering this aspect, the configuration can be simplified as shown in Fig. 3.7 (b). In this case, the error signal *e(t)* is further offset by 90° by means of a "all-pass" filter [24]. Thus it is necessary to provide only the reference signal $\sin(\omega_r t)$ and ω. The "all-pass" filter is easy to implement in the z-domain and is less sensitive to the effects of quantization having the order of one [119]. The characteristic equation with finite differences is (3.13) [24]:

$$y[n] = Ay[n-1] + Bx[n] - x[n] \tag{3.13}$$

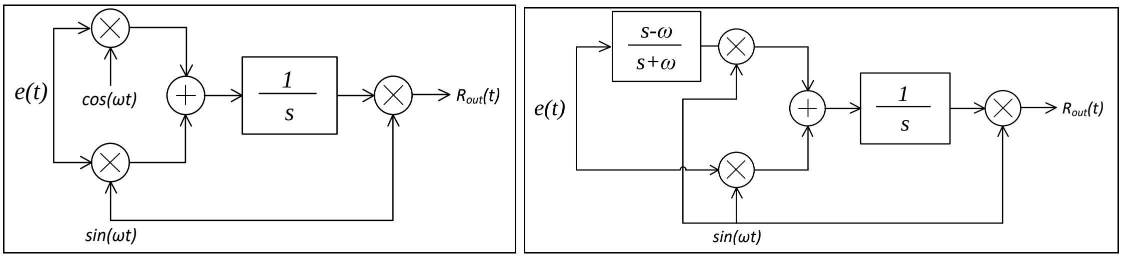

(a) *(b)*

Fig. 3.7 Resonant term implemented using a phase-sensitive amplifier (a) and his simplified form (b)

In case the phase error input by the output filter is low, the resonant term can be implemented using the topology of Fig. 3.8 (a). According to (3.11) and (3.12) the continuous component at the output of the propagation circuit depends on the phase difference between the e (t) and sin (ωt) signals. To maximize the continuous component, the phase difference between the two signals must be zero. The compensation of any phase errors introduced by the controlled system can be done using "all-pass" phase filters as shown in Fig.3.8 (b). The additional phase introduced by the "all-pass" filter is estimated by:

$$\angle H_{AP}(s) = 180 - 2\tan^{-1}\left(\frac{\omega}{\omega_0}\right) \tag{3.14}$$

Where ω_0 is the own frequency of the "all-pass" filter.

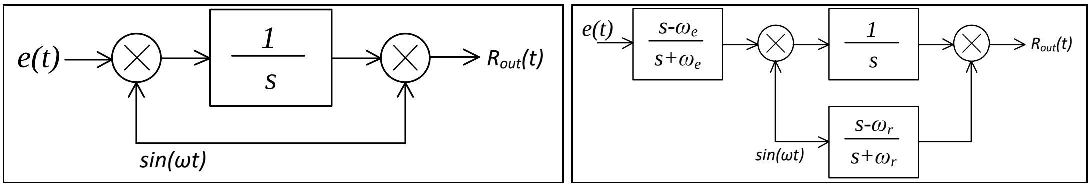

(a) *(b)*

Fig. 3.8 The simplified resonant term (a) and how the phase errors can be compensated using "all-pass" filters

The major advantage of implementation based on the phase-sensitive amplifier is the low sensitivity to the quantization errors associated with the filter coefficients that are part of the resonant term. Practically, the performance depends on the accuracy of the $sin(\omega_r t)$ reference signal. If this type of control is basically implemented using a low cost *DSP*, fixed bit 16 bit, it can be a major advantage. There is also a disadvantage of this implementation: the calculation of the *sin(ωt)* reference in real time requires important resources. This may become a major problem if there are several resonant terms requiring different frequency reference signals, such as *APFs*. For the case of fixed-point processors, trigonometric functions are calculated using tables; so the required calculation time is very low.

For high-power applications in industry, the costs associated with using a powerful floating-point *DSP* are not a major issue.

3.2.4. The Effects of Noise

Converting the control parameters from the s domain into the z range is done by means of an analog-to-digital converter *ADC*. It also introduces adverse effects that need to be taken into account in a real implementation. The first effects are introduced by the sampling and quantization processes taking place in *ADC*s.

The noise distribution is considered to be uniform in the range $-\Delta_N/2$, $\Delta_N/2$ where Δ_N is the quantization interval. The statistical average of the error signal defined as $e_n=Q[x(n)]-x(n)$ is zero. The variance of the error is:

$$\sigma_Q^2 = E[{e_n}^2] = \frac{\Delta_N^2}{12} \tag{3.15}$$

For a 10-bit *ADC*, the theoretical dynamic range is about 60 dB. In practice, the noise input by processes associated with the power converter (switching power elements, parasitic resonances, etc.) can reduce this dynamic range. *DSP*s developed for power applications generally include an *ADC* with a resolution of between 10 and 16 bits. The preferred converter type is the one with successive approximations due to low cost and high speed. The presence of *ADC* within the *DSP* is conditioned by constraints related to the time of sampling; a timing synchronization signal is generated by the integrated *PWM* generator. Figure 3.9 (a) shows the optimal ranges in which the sampling process can take place. Practically, this range imposes restrictions on sampling frequency; the sampling frequency must be an entire submultiple of the switching frequency. In the optimal case the two frequencies coincide.

In [27] it is shown that in the case of sinusoidal signals the estimated variance of (3.15) is not correct. In this case, a modified relationship is needed to correctly estimate this parameter:

$$\sigma_Q^2 = \frac{1}{12} + \frac{1}{\pi^2}\sum_{n=1}^{\infty}\frac{(-1)^2}{n^2}J_0(2\pi n A) \tag{3.18}$$

Where J0 is the *Bessel* function of the order 0 and *A* is the amplitude of the sinusoidal signal.

Fig.3.9 (b) shows the variance of error according to the amplitude A of the sinusoidal signal. For large signal amplitude values the variance can be precisely approximated using (3.15). When the signal amplitude decreases, the variance of the quantization error differs significantly from the estimated value by (3.15). To minimize the errors introduced by the quantization process it is necessary to maximize the amplitude of the applied signal at the *ADC* input so that in all cases it is within the upper limit of the accepted range.

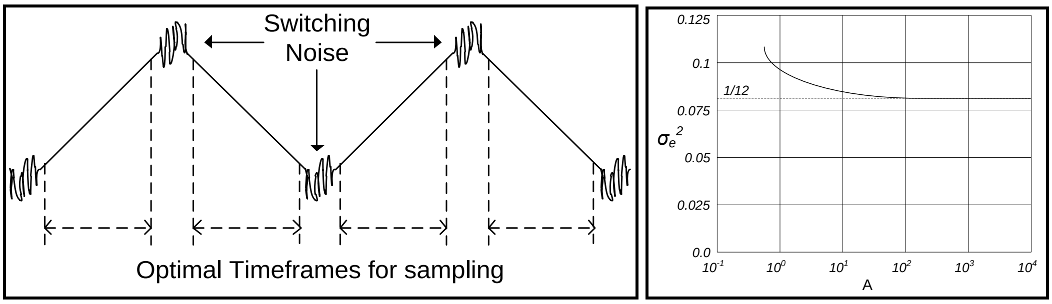

(a) *(b)*

Fig.3.9 Optimal timeframes for sampling (a) and the variance of the error as a function of signal's amplitude A (b)

3.2.5. Conclusions

Implementing the PR controller in the z-domain is of particular practical importance because of the benefits it offers. Among these advantages can be mentioned: increased flexibility, extremely tight tolerances of parameters, lack of effects caused by environmental factors such as temperature and the inherent aging of components. However, there are a number of adverse effects associated with this implementation that need to be considered to ensure a correct estimate of the controller's performance. The main effects are related to the process of quantization, inevitably in digital implementation. The resonant term of the PR controller has two conjugated complex poles whose frequency is equal, making it extremely sensitive to quantization errors of the equivalent digital filter coefficients. The simulations made lead to the conclusion that it is virtually impossible to implement such a controller using a 16-bit fixed-point *DSP* (low cost). A solution has been proposed to solve this situation, namely to implement the resonant term using a phase-sensitive amplifier. The proposed solution allows the implementation of the PR controller using low-cost DSPs specifically developed for power applications.

The effects of the noise on the controller were also discussed, demonstrating the impossibility of obtaining the estimated performance by using models in the s-domain and the extremely high resolution of the simulators operating in this domain.

3.3. The Time Response of the PR Controller

The above-described topologies can be used to implement resonant control especially when it is desired to verify the application using a simulator in the s-domain. Assessing the controller's stability and its response to the unit step input are essential steps in the design stage. It is also important to evaluate the effects of the final gain of the resonant term; in a real implementation the gain is finite and depends on the resolution of the control system.

3.3.1. The Effects of a Non-zero Damping Ratio

Consider the PR controller described by (2.12). This is the popular form found in most of the specialist articles. The response to a sinusoidal excitation signal as well as the unit step response will be evaluated by simulation. For simplicity, K_P=1. Also K_R is constant, 10. Simetrix/Simplis is used for analysis. The resonance frequency is 50 Hz in all cases.

In [12] it appears that it is not advantageous to introduce a damping factor because infinite gain does not affect the stability of the controlled system; the point of interest where stability is assessed is where the gain of the loop is unitary and the position of this point depends on the characteristics of the controlled system, not the controller. However, this article discusses only the frequency response, not the time response. In Fig. 3.11 shows the replies to the original version step implemented with two ideal integrators and the version proposed by the author. A 50 Hz sinusoidal signal is applied for one second. It is noted that for the ideal resonant term the output remains constant after removal of the stimulus. In the case of the modified resonant term, the output exponentially converges to zero after the stimulus is removed.

To evaluate the effects of the resonant response time on the performance of the controlled system, a single-phase inverter model is used where the output current is controlled using a *PR* controller. For this model the parameters are: 20 kHz switching frequency, coil inductance 1 mH, load resistor 1 Ω. For the first set of simulations, the controller parameters are: $K_P = 1$, $K_R = 1$ and $\xi = 10E\text{-}5$. The following parameters are displayed: reference voltage for the Vref controller, current in inductor IL, output of the proportional term P_Out and output of the resonant term R_Out. In Figure 3.12 these parameters are displayed as a result of the simulation. The exponential response is observed at the resonant term output after applying the step-type signal. In the first part of the interval the proportional term dominates the controller output and ensures the follow-up of the Vref reference. The response time for the resonant term output signal is long, many periods of the reference signal being required to compensate for the stationary error. When the amplitude of the reference signal is significantly reduced, the output of the resonant term has a high amplitude and due to the very low damping factor it decreases with a very long time constant. This introduces an undesired additional phenomenon, namely a controlled signal error; In this case, the inductor current has an alternate component whose amplitude is not controlled by the reference. This error is present in the waveforms presented in Fig.3.12.

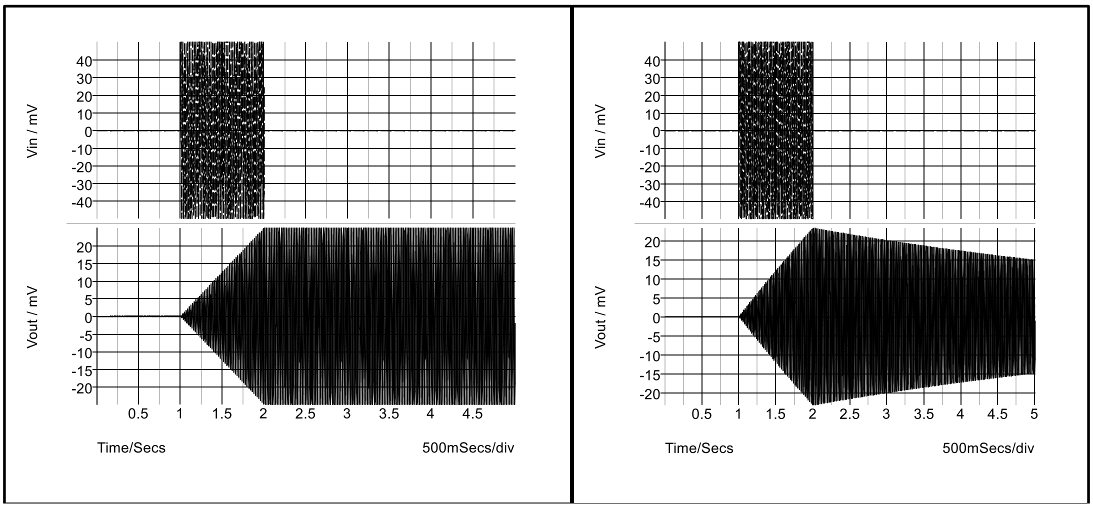

Fig. 3.11 Step response time response for the original resonant term (low damping factor) and for the modified one (larger damping ratio)

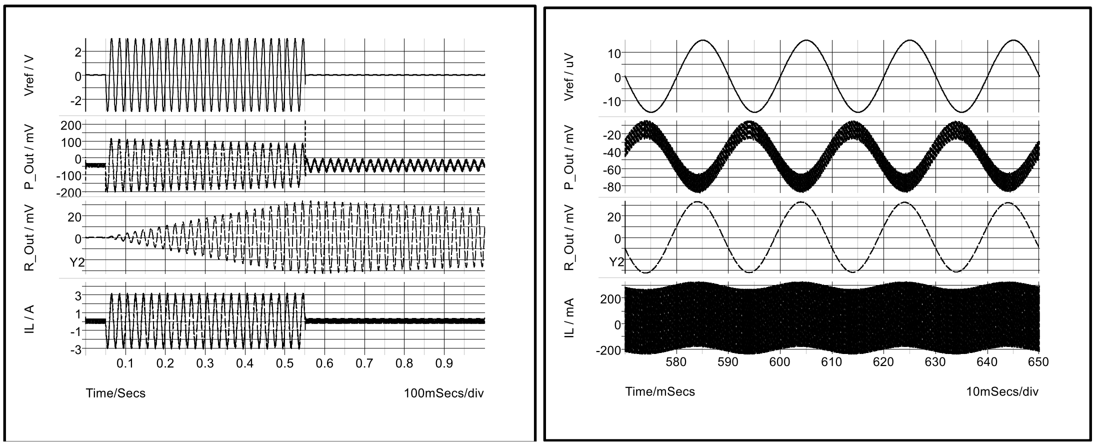

Fig.3.12 The time response of the inverter (ξ=10E-5) and the transient error introduced by the response of the resonant term

For the quantitative analysis of the stationary error introduced by the finite gain of the resonant term, a model of the controlled system is used. The block diagram of the closed-loop system is shown in Fig.3.33 (a). The inverter is modeled as a first order system:

$$H_{INV}(s) = G_{PWM}\frac{1}{sL+R_L} \tag{3.44}$$

Where L is the output filter inductance, R_L is the load resistance and G_{PWM} is the gain of the PWM modulator. G_S is the gain of the current sensor that measures the current in the inductor.

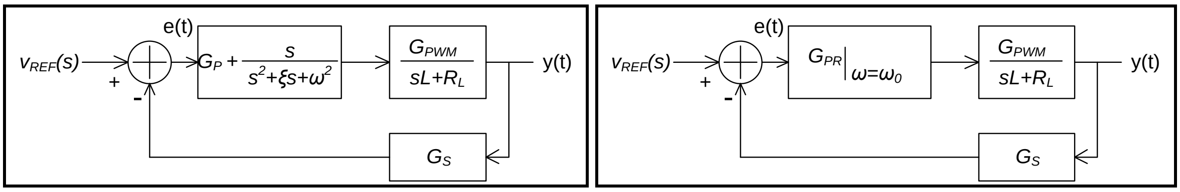

(a) *(b)*

Fig.3.13 Closed loop system's model, the complete one (a) and the simplified one (b)

To evaluate the stationary error in the negative feedback control systems, refer to the final value theorem [32]. For a given system the stationary error is:

$$e_f(s) = \lim_{s\to 0} sE(s) \tag{3.46}$$

Where e_f is the stationary error (t→∞) and *E(s)* is the error in the control system calculated as the difference between the reference signal and the actual output at the system output.

The stationary error evaluation is done by applying an impulse type, step unit, ramp or accelerated ramp to the input of the system and evaluating (3.46). For the case of the PR-controller with sinusoidal input this theorem cannot be applied because the conditions of existence for (3.46) are not met. The resultant equation for which the limit is to be evaluated is a pair of poly complexes, in which case the final value theorem does not apply. Also, the final value for a sinusoidal signal cannot be defined. In order to apply this theorem to the PR controlled system, some initial assumptions are required:

- The gain of the resonant term is finite. This is ensured by the non-zero damping factor.
- The system is now controlled by a "proportional" controller whose gain is given by the gain of the *PR* controller rated for the resonance frequency.
- The applied stimulus is a step unit.

Figure 3.13 (b) presents the new system resulting from the above simplifying assumptions. For this result system the application of the final value theorem leads to:

$$e_f = \frac{1}{1+\frac{G_S G_{PR} G_{PWM}}{R_L}} = \frac{R_L}{R_L + G_S G_{PR} G_{PWM}} \tag{3.53}$$

Stationary error is nonzero for any finite G_{PR} gain. A high gain reduces stationary error; in the case of an ideal integrator this gain is infinite, the stationary error in this case being null. The gain of the resonant term amortized at the resonance frequency can be calculated as follows:

$$G_{PR}(\omega_0) = \left|\frac{s}{s^2+\zeta s+\omega_0^2}\right|_{s=j\omega_0} = \frac{1}{\zeta} \tag{3.54}$$

3.3.2. Conclusions

In real implementation the gain of the resonant term is always finite. This implies a non-zero stationary error. Basically the system is controlled by a proportional controller and its stationary error can be estimated using the finite value theorem.

The time response to the unit is strongly dependent on the damping factor. A low damping factor makes the response of the resonant term very long by introducing additional errors if the reference signal suddenly decreases from the steady state value to a considerably lower value. Increasing the damping factor reduces the response time of the resonant term to the unit but decreases its gain by increasing the stationary error.

4 The Control of Power Converters Using PR Controllers

This chapter investigates the use of *PR* control for power converters that work with time-varying reference signals. This type of control will be evaluated for several types of power converters such as inverters, *APF*s and *PFC* circuits using simulations in the s-domain. The simulation models will be developed using *PSIM* and *Simetrix/Simplis* simulation environments.

4.1. The Control of Inverters

Performance evaluation is done using a model developed in *PSIM*. In this case, the controlled parameter is the average current of the output inductor corresponding to the current supplied in the inverter load. The average value of current control will be implemented using three types of controllers in the stationary reference system. The three types of controller used are: *P* type, *PI* type and *PR* type. The type of modulation used is the "bipolar" type with a carrier frequency of 20 kHz. The gain of the current sensor that measures the current i_L is unitary.

In Fig. 4.1 (a) shows the output current (i_L) of the single-phase inverter when using a P-type controller with unitary proportional gain. There is a consistent stationary error. Reducing this stationary error is by increasing proportional gain. Fig. 4.1 (b) presents the stationary error if the proportional gain is 20 dB. The increase in the proportional gain to 46 dB significantly reduces the stationary error value (Figure 4.2), but the *PWM* modulator operation is affected by the presence of the ripple in the control voltage.

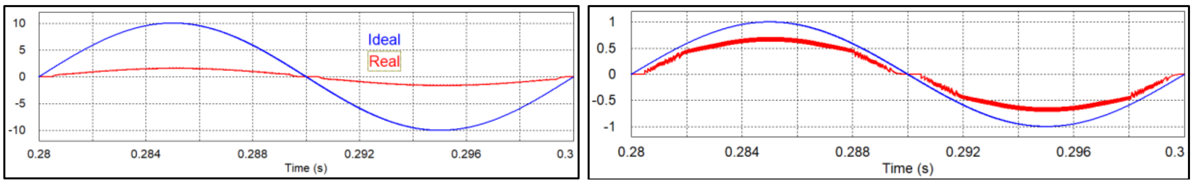

(a) *(b)*

Fig. 4.1 The reference and the real waveforms of the inverter's output current. The controller is of P type (GP=0 dB (a), GP=20 dB (b))

The next type of controller applied is *PI* type. The associated transfer function is:

$$H_{PI}(s) = \frac{1+\tau s}{\tau s} \tag{4.1}$$

Where τ=0.001s.

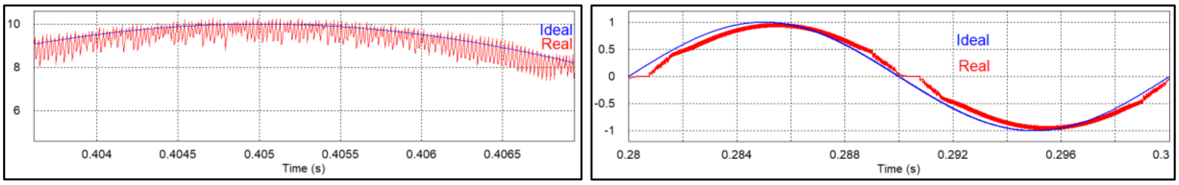

Fig. 4.2 The stationary error of a P controller (GP=46 dB) and the same error for PI controller

In this case, the presence of the stationary error and the presence of a phase error are observed, the controller not being able to follow the required reference. This additional phase error can significantly affect the performance of the inverter if it is connected in parallel with the network by reducing the power factor. Increasing the proportional gain reduces the phase difference but negatively affects the operation of the *PWM* modulator.

For the next set of simulations, enter the *PR* control. The *PR* controller used for inverter control is described by:

$$H_{PR}(s) = 1 + \frac{s}{s^2 + 0.01s + (2\pi 50)^2} \tag{4.2}$$

In this case, the proportional gain is unitary and the gain of the resonant term is finite, equal to 40 dB at the resonance frequency. The waveform of the output current is shown in Fig.4.3. The stationary error is substantially reduced without affecting the operation of the *PWM* modulator. *THD* is excellent, about 4.4%.

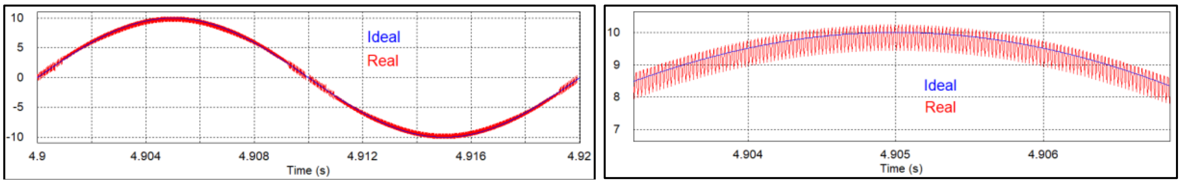

Fig. 4.3 The inverter's output current waveforms and the stationary error in the case of PR controller

Previous simulations demonstrate the superior superiority of resonance control over classical solutions based on *P* and *PI* controllers. In the following, the performance of the resonant control will be evaluated if the load at the inverter output is nonlinear. For the first set of simulations the load connected to the output consists of a full-wave rectifier followed by a 4700 µF capacitor filter and a 10 Ω resistor. The controller used is the one described by (4.2). The output current and its spectrum are shown in Fig.4.4. In this case *THD* is 33% and the spectrum is dominated by the fundamental and its odd harmonics, especially the third and fifth.

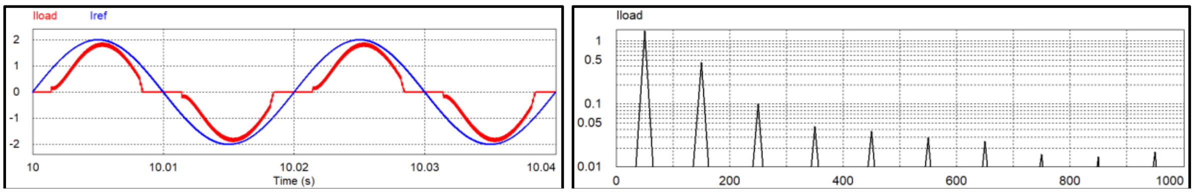

Fig. 4.4 The output current and his spectrum in case of the nonlinear load

The introduction of an additional resonant term granted on the third harmonic frequency leads to a *THD* of 24%, a decrease of about 9% compared to the previous case where a single resonant term was present. The output current and its spectrum are shown in

Fig. 4.5. In this case the gain of the two resonant terms is equal to 40 dB at the associated resonance frequencies. It notes the low amplitude of the third harmonic.

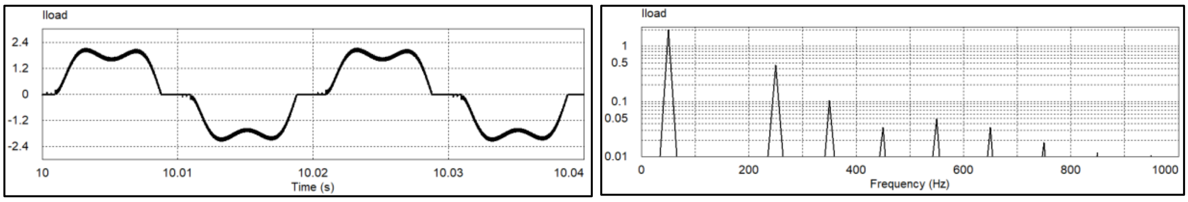

Fig. 4.5 The waveform of the output current and his spectrum. The load is nonlinear and the control is PR with two resonant terms (50 Hz and 150 Hz)

4.1.3. The Hybrid Control

Resonant control of inverters allows for excellent performance and can successfully replace classical control based on *P* and *PI* controllers in StRS or *PIs* in ScRS. The cost of implementing resonance control is generally higher than classical solutions using dedicated integrated circuits because it requires the use of a *DSP*. A low-cost solution that can be used to control simple inverters that are part of the *UPS* is based on a hybrid control system. Within this system the resonant controller is implemented in the s-domain and output is controlled by a digital *PWM* modulator that is part of a digital system. The reference signal is generated by the digital system using a Digital-to-Analog Converter (*DAC)*. Implementation of this topology can be done using 8-bit microcontrollers whose cost is very low by comparing the costs associated with a dedicated *DSP*.

The block diagram of the proposed hybrid controller is shown in Fig.4.6. The *PR* controller is implemented in the s-domain using one of the topologies presented in the previous chapter. The reference signal is generated by the microcontroller using the internal DAC converter and a *Numerically Controlled Oscillator* (*NCO*). The amplitude of the output voltage of the inverter is controlled in the closed loop by altering the amplitude of the reference sinusoidal signal. The signal from the *PR* controller output is passed to the z-domain with the internal *ADC* converter and directly controls the digital *PWM* generator inside the microcontroller. Thus, a low cost microcontroller can be used to implement a resonant control system for *UPS*.

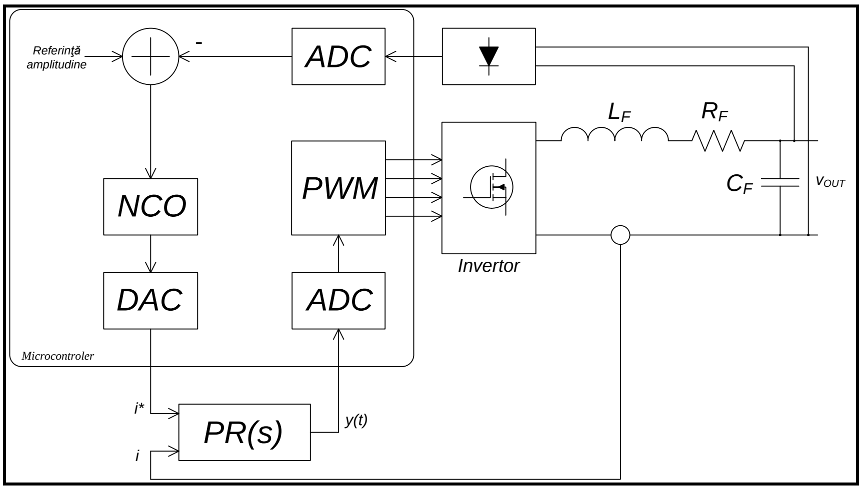

Fig. 4.6 The block diagram of the hybrid controller

4.1.4. Conclusions

The use of resonant control for inverters brings substantial benefits for both linear loads, by reducing stationary error, especially for nonlinear loads where it ensures the selective elimination of harmonics in StRS without resorting to coordinate changes. The relatively high cost of z-domain implementation is justified by the performance achieved. For low cost applications where the reference signal frequency is fixed, hybrid control may be used in which the implementation of the *PR* controller is made in the s-domain using operational amplifiers and passive components.

4.2. The Control of Active Power Filters

In order to evaluate the performance of the *AFP*s, the *PSIM* model presented in Annex A was developed. The performance of the different control methods based on *PI* and *PR* type linear controllers.

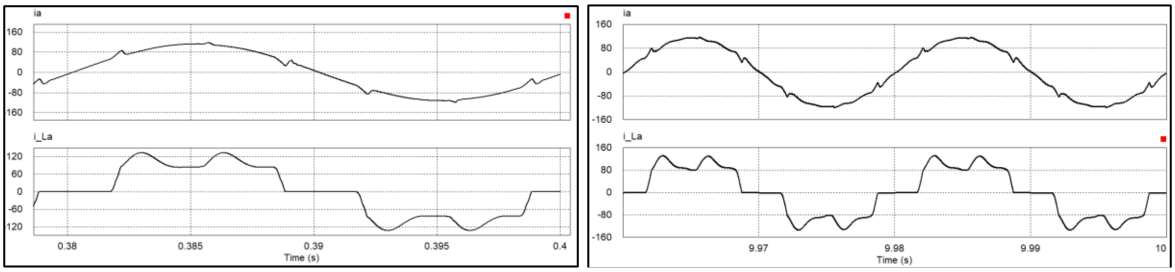

Fig. 4.7 The line and load current of a three-phase APF controlled by a PI respectively PR controller

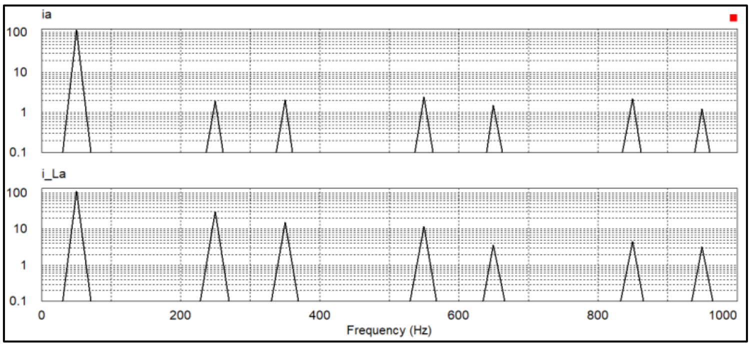

Fig. 4.8 Spectrum of the line and load current (PI controller)

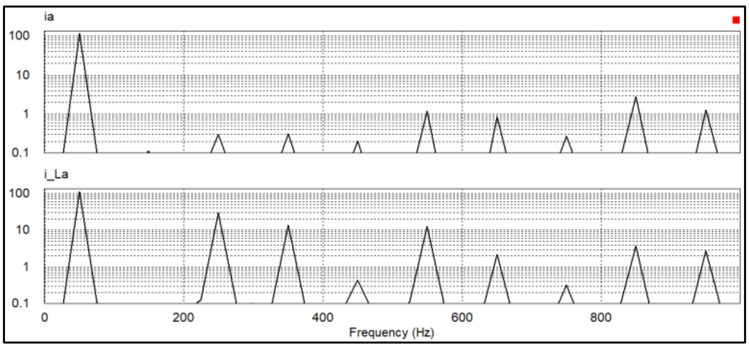

Fig. 4.9 Spectrum of the line and load current (PR controller)

4.3. The Control of Power Factor Correction Circuits

In Fig. 4.10 presents a classic implementation of a PFC based on a Boost converter. This configuration is widespread and is used for power factor correction in both three-phase and single-phase systems. It is also the basic configuration for deploying low-distortion rectifiers in general-purpose AC-DC converters in the industry as well as in consumer goods. For the first set of simulations, the *PI* controller is used. This is the usual configuration found in most PFC applications. The *PI* controller is described by:

$$H_{PI}(s) = 0.5\frac{1+\tau s}{\tau s} \tag{4.15}$$

Where τ= 0.0001 s.

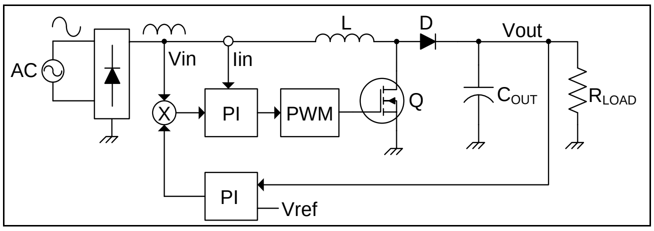

Fig. 4.10 PFC circuit implemented with a Boost-type converter

The performances of the low distortion rectifier based on the *Boost* converter and controlled by the *PI* controller are generally very good. However, the *Boost* converter is very sensitive to noise and in high power applications where the switching frequency is relatively low, it is desirable to reduce the level of high frequency ripple inserted in the PWM modulator. Thus, the controller's band must be severely limited to just a few kHz. This bandwidth has a negative impact on the tracking capability of the reference signal. In this case, a resonant time can be given on the fundamental frequency of the reference signal, respectively, 100 Hz in this case. The controller contains two terms, a P-type with limited band and a resonant one on the frequency of interest. The proportional term may be replaced by a PI-type term where the bandwidth limitation is inherent.

The transfer function of the proposed controller is:

$$H_{PR}(s) = K_P\frac{\omega_P}{s+\omega_P} + K_R\frac{1}{s^2+\omega_R{}^2} \tag{4.16}$$

where K_P = 26 dB, K_R = 0 dB, $\omega_P = 2\pi 700$ and $\omega_R = 2\pi 100$.

Fig.4.11 shows the input current spectrum for the two control strategies. One can notice a significant decrease in the amplitude of the third harmonic when using the resonant term.

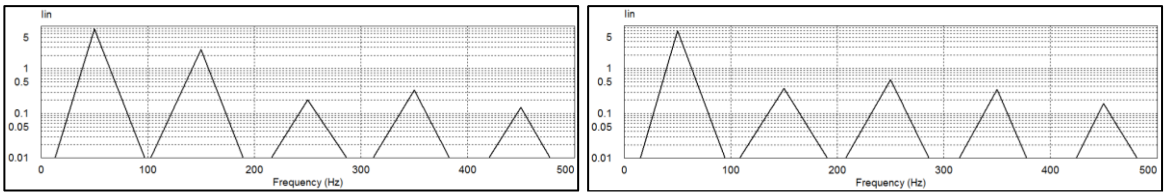

Fig. 4.11 Input current spectrum for a PFC circuit controlled by PI respectively PR controllers

PFC circuits based on the low distortion rectifier implemented with the *Boost* converter also benefit from improved performance if resonant control is used. The introduction of a single resonant term in parallel with the classical *P* or *PI* controller can significantly reduce the magnitude of the dominant harmonics, especially where there are constraints related to the maximum switching frequency. The resonant term also provides minimal protection against the noise input by the reference signal which is taken over by the input voltage. This control strategy was proposed in [O.1].

4.4. The Stability of the Control System

Assessing the stability of the control system is an important step in the design stage of the power converter. The *PR* controller belongs to the family of linear controllers for which stability analysis is done using specific techniques such as the *Nyquist* criterion and the *Bode* diagrams.

The inverter of Fig. 2.7 is considered to be the transfer function (2.2). The related controller contains a proportional term and three resonant terms given on the 50 Hz fundamental frequency, respectively on the 3rd and 5th harmonics. The closed-loop system diagram is shown in Fig.4.12.

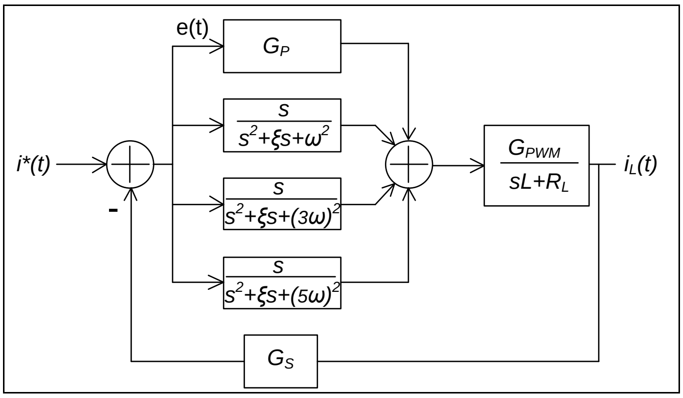

Fig. 4.12 The block diagram of the closed loop system

The system's closed loop transfer function is:

$$G_{CL}(s) = \frac{G_F(s)}{1+G_S(s)G_F(s)} \tag{4.17}$$

Where $G_F(s)$ is the direct path transfer function and is given by:

$$G_F(s) = \frac{G_{PWM}}{sL+R_F}\left(G_P + \frac{s}{s^2+\zeta s+\omega^2} + \frac{s}{s^2+\zeta s+(3\omega)^2} + \frac{s}{s^2+\zeta s+(5\omega)^2}\right) \tag{4.18}$$

For the characteristic polynomial of this transfer function, the *Bode* or *Nyquist* diagrams can be drawn and stability can be assessed using known criteria. The high complexity of the transfer function makes it difficult to use analytical techniques. Generally because of the large order of the characteristic polynomial (in this case the polynomial is of the order of seven), the analytical methods that require finding the solutions are difficult to apply. Graphics such as *Bode* diagrams provide important information about both stability and important additional parameters such as the control system bandwidth.

4.4.1. Conclusions

System stability assessment is a fundamental step in the design of applications involving controlled power converters using resonant controllers. In order to evaluate stability, we use the techniques devoted to linear and invariant systems in time such as the Bode and Nyquist diagrams. This is a major advantage of PR controllers compared to nonlinear methods used in the past.

5 Practical Results

To implement the PR controller proposed in Chapter 3, a flexible hardware platform consisting of a single-phase inverter and a control and control board has been developed. The control and control board enables the implementation of resonant control in both the s and z domains.

5.1. Hardware Platforms

In Fig. 5.1 shows the image of the inverter and the output filter. The two subassemblies are interconnected using the J2 connector placed on the inverter board. Input voltage to the inverter is supplied from outside using the J1 connector. The input voltage range is between 0 V and 400 V and the maximum current supplied by the inverter is 5 A_{RMS}. The digital control system is implemented using a dsPIC33FJ16GS502 DSC produced by Microchip Technology. This DSC is especially developed for controlling power converters. The DSC is powered at a 3.3 V voltage supplied by a voltage regulator MCP1703-3 on the control and control board. Analog inputs are used to measure the current sensor output voltage, output voltage of the inverter output voltage measurement circuit, and output of the PR controller implemented in the s range. The control signal for the power switches is provided by the PWM generator integrated digital. Also, the same PWM generator provides the "dead time" required for the optimum command of the power switches.

The analog PR controller is implemented using the topology described in Fig. 3.6. A "double T" network is inserted into the negative feedback loop of an operational amplifier. The output of the "double T" network is isolated from the inverse input of the operational amplifier (low impedance node) by means of a repeater amplifier. Within the "double T" network, passive components, resistors and capacitors with 5% tolerance were used. The capacitors used are high-quality PPS (Polyphenylene sulfide) film type. The reference for the analog PR controller is provided by the DSC at the non-inverting input of the operational amplifier. This also produces the generation of the "error" signal by the same functional block, respectively the operational amplifier. The control board and the inverter board are interconnected using the J2 or J5 connectors. The assembly of the two plates is shown in Fig. 5.1 (c).

(a) *(b)* *(c)*

Fig. 5.1 The inverter (a), the output filter (b) and the inverter-control board assembly (c)

5.2. The PR Controller in s-domain

The performance evaluation of the PR controller implemented in the field is done by performing measurements in the frequency domain using the Bode 100 analyzer and in the time domain using the signal generator and the oscilloscope.

The resonance frequency measured using the Bode 100 type analyzer is approximately 51.6 Hz, an acceptable deviation considering no effort has been made in choosing components with tight tolerances. The capacitance measured by a RLC bridge is 488 nF, a 3.8% deviation from the nominal value of 470 nF. The gain at the resonance frequency is about 50 dB and the quality factor is relatively low, as shown by the simulations in Chapter 3.

In Fig. 5.2 the input and output signals of the PR controller are presented. The input signal has an amplitude of about 2.5 mVpp and the output signal is about 0.83 Vpp. The gain determined under these conditions is 50.4 dB, very close to the value measured by the Bode 100 analyzer.

The time response to the unit step signal is shown in Fig.5.3. There is a similarity with the behavior of the simulations in Chapter 3.

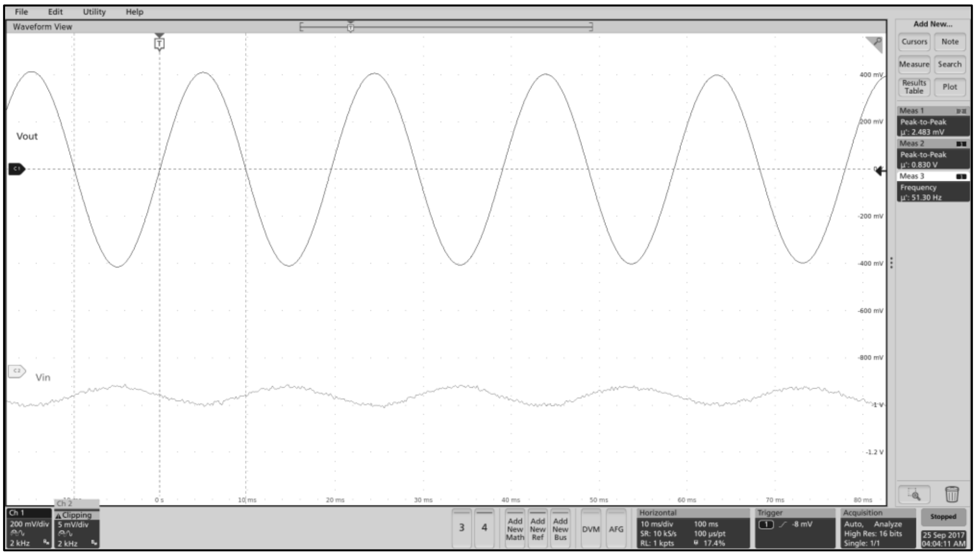

Fig. 5.2 The input and output voltages of the s-domain PR controller

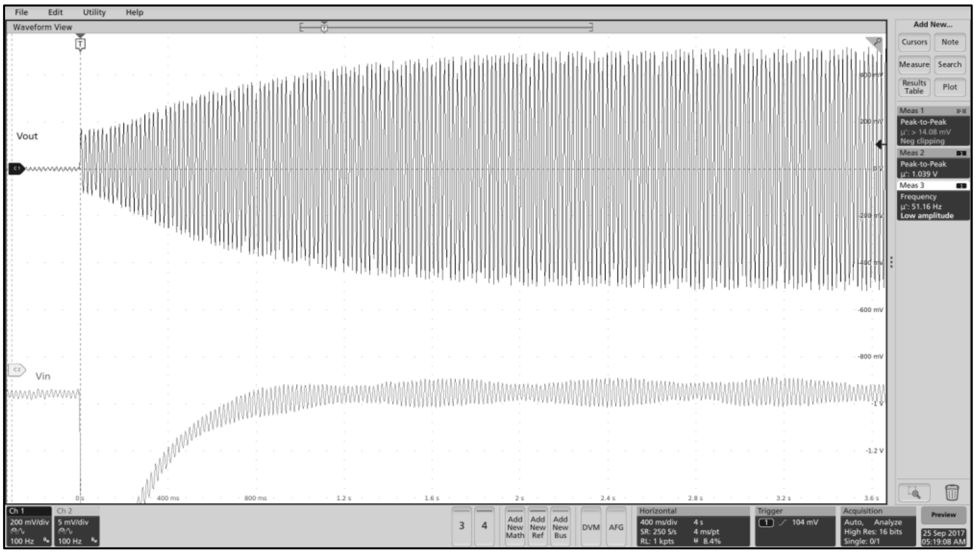

Fig. 5.3 The time response of the s-domain PR controller

5.3. The Control of Single-phase Inverter

The next set of tests is performed on the single-phase inverter using digital control and various types of outputs connected to the output. Both the output current spectrum and the response to the variation of some external parameters such as the inverter input voltage.

A 10 Ω resistor with a maximum power dissipation of 50 W is used as a load for the single-phase inverter to evaluate the performance of the PR controller in the case of linear loads. The supply voltage of the inverter is between 20V and 60V supplied by an adjustable laboratory source. The switching frequency is fixed at 20 kHz, and the type of PWM modulation used is symmetrical with a triangular carrier. Resonant terms are introduced sequentially and the effects of these terms are observed on the output current spectrum. The results are presented in Figures 5.4 and 5.5.

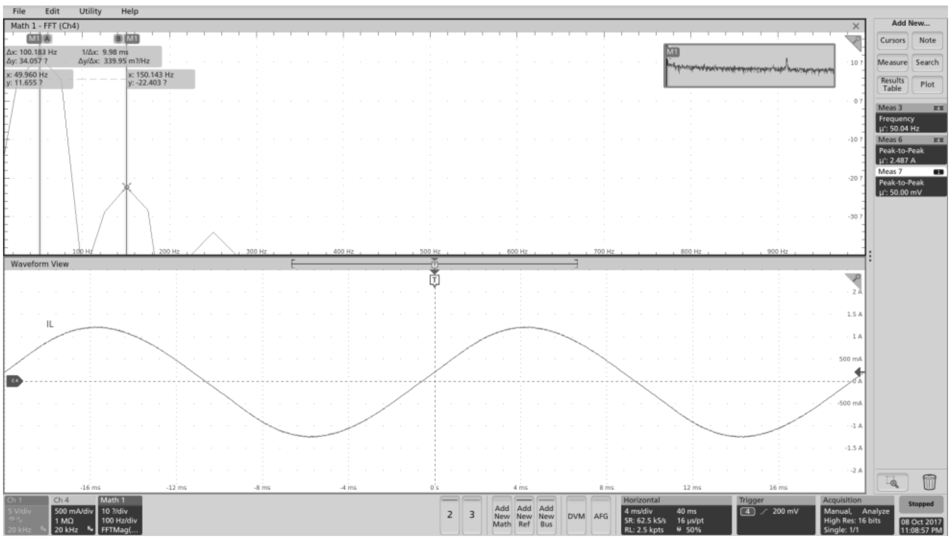

Fig. 5.4 Inductor's current spectrum; the control is of PR type with a single resonant term (50 Hz)

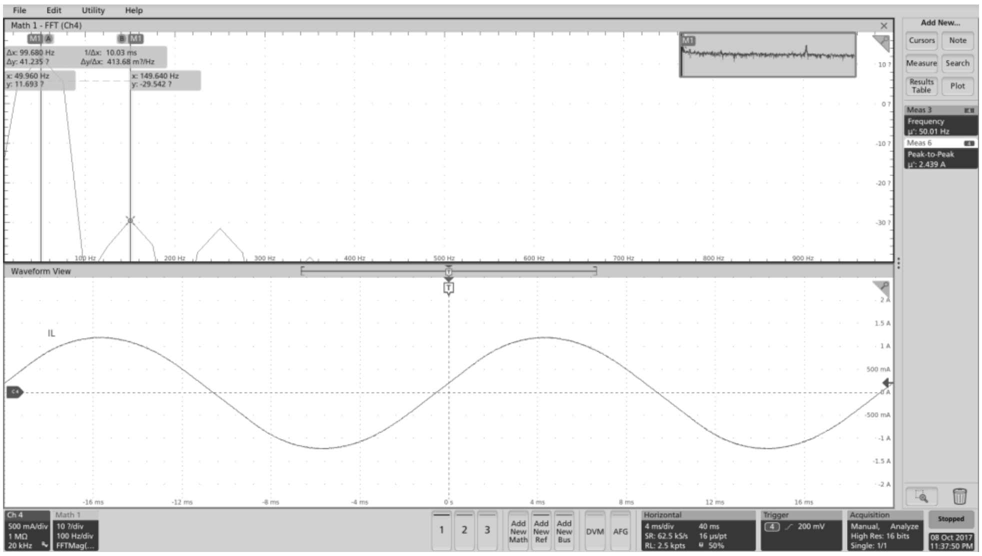

Fig. 5.5 Inductor's current spectrum; the control is of PR type with two resonant terms (50 Hz and 150 Hz)

The nonlinear load consists of a single-phase full-wave rectifier followed by a capacitor of 4700μF. The rectifier's load is the same 10Ω/50W resistor. For the first tests, the PR controller is used with a single resonant term tuned on the fundamental frequency and unitary proportional gain. The spectrum of the output current in this case is shown in Fig.5.6.

For the next set of tests, the additional resonant terms assigned to the frequencies corresponding to the third, fifth and seventh harmonics are introduced sequentially. The results obtained are presented in Fig.5.7. It is noted the selective elimination of dominant harmonics by the high gain of the controller at the frequencies corresponding to these harmonics.

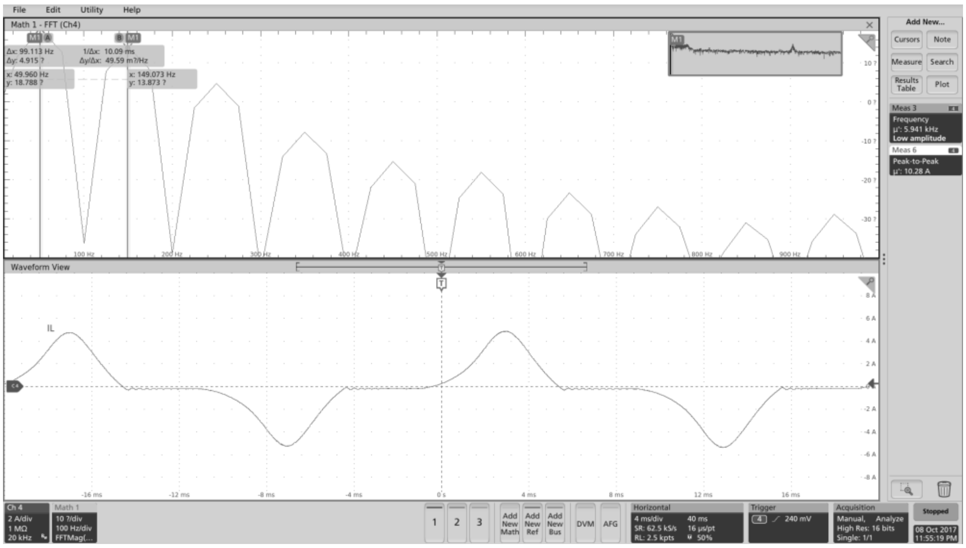

Fig. 5.6 Inductor's current spectrum; the load is nonlinear and the control is PR-type with a single resonant term (50 Hz)

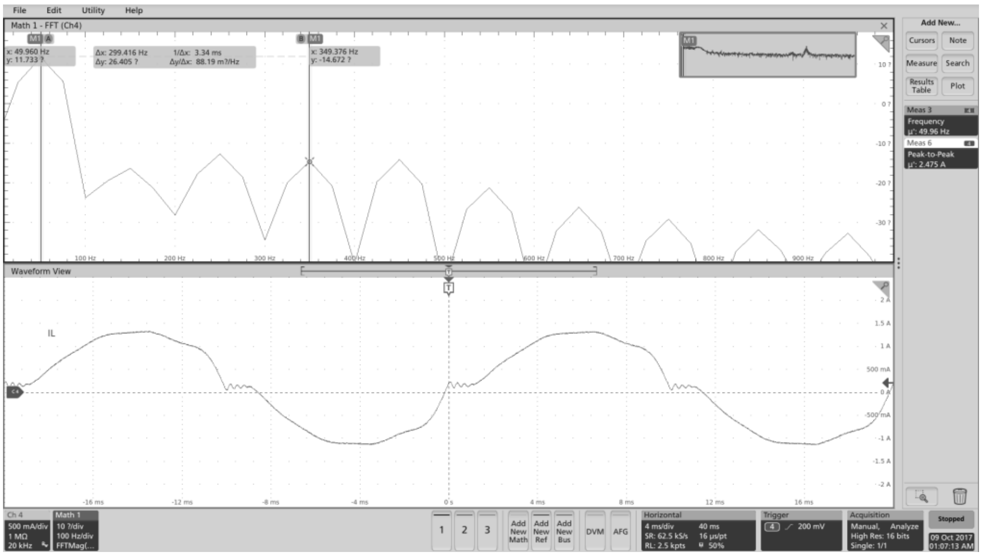

Fig. 5.7 Inductor's current spectrum; the load is nonlinear and the controller is PR-type with four resonant terms (50 Hz, 150 Hz, 250 Hz, 350 Hz)

The evaluation of the response to the unit step signal is in the first case by varying the supply voltage of the inverter and monitoring the effect on the controlled parameter, i.e. the output current. The load used in this case is linear (10Ω/50W) and the *PR* controller contains only one resonant term on the fundamental frequency. The response of the *PR* controller to the sudden change in supply voltage from 30V to 60V is shown in Fig.5.8. There is a long response time similar to that obtained from the simulations.

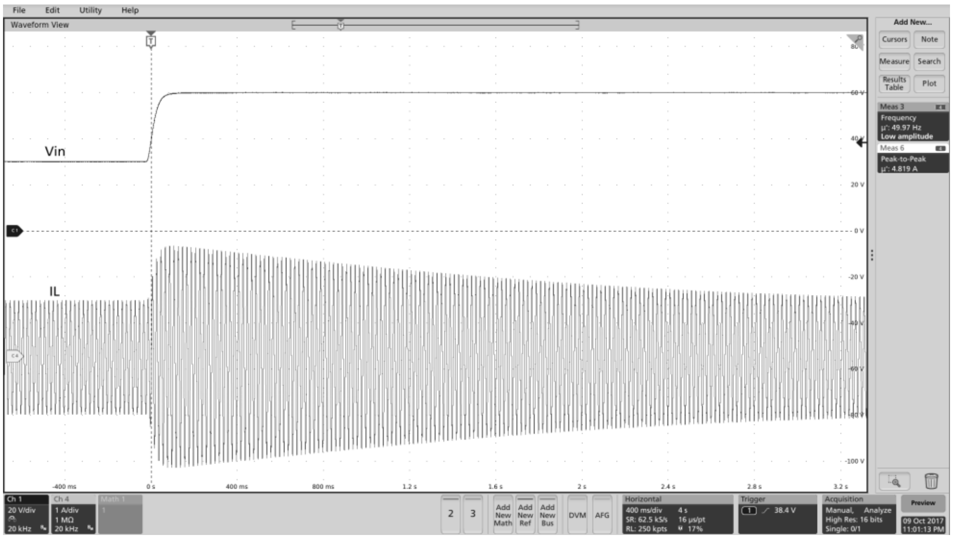

Fig. 5.8 Time response of the controller at the variation of the input voltage

5.5. Conclusions

The PR controller provides excellent performance when used to control power converters requiring variable reference signals. These performances are confirmed by the tests performed on the hardware platform implemented for this purpose. The practical results closely match the results obtained from the simulations.

Among the advantages of PR control can be remembered:

- The *PR* controller operates in StRS. This is a fundamental advantage that greatly reduces the complexity of the control system; there is no need for many coordinate changes, especially for three-phase systems.
- High gain at resonant frequencies. In practice, stationary error for spectral components that coincide with resonant frequencies is null (very low in case of real implementation).
- Resonant terms are selective by ensuring excellent noise rejection. High performance is achieved using a low proportional gain, thus reducing the sensitivity of the controller to the noise input of the power converter.
- Selective elimination of harmonics, very important for *AFPs*, is very easy. Practically, resonant terms are introduced on harmonic frequencies to be eliminated.
- The *PR* controller belongs to the family of linear controllers. Thus, for the analysis of PR control systems, simple methods, such as the *Bode* and *Nyquist* diagrams, can be used.

The simplified implementation method proposed in 3.3 makes it possible to carry out the PR controller using low-cost, 16 bit fixed-rate DSPs. This opens the way for developing advanced applications where the cost of implementing and analyzing the control system is kept under control. The measured performances for this type of implementation are excellent; the stationary error for controlling the output current of a single-phase linear load inverter is approximately 0.6%

In case the final cost of the application has to be very low, as is the case with UPS for commercial use, hybrid control can be implemented. The usefulness of this type of control, relatively limited due to the tolerances of the passive components used in the implementation, was confirmed by the practical tests.

6. Conclusions

6.1. Achieved Results

In Chapter 2 were presented the usual control methods for power converters with variable reference signals: hysteretic control and *Sliding Mode* control, both belonging to the nonlinear control family, the *PI* type controller in the synchronous reference system, the type controller *Vector PI*, repetitive controller and *PR* resonant controller. For each method, the advantages and disadvantages as well as the reference system in which the controller operates are specified. The chapter concludes with a series of conclusions about the most important control methods related to the resonant *PR* controller. This method is considered by the author as the modern method of control for said power converters providing both excellent performance and outstanding simplicity in terms of practical implementation and theoretical analysis.

Chapter 3 discusses the implementation of *PR* resonance control in the two fundamental domains, s respectively z. Five analog circuitry topologies that can be used to implement the PR controller in the s domain are proposed. These circuits can be used to simulate the converter using simulators that operate exclusively in the continuous time domain as well as to implement hybrid resonance control for cost applications low. In terms of z-domain implementation, the effects limiting the performance of this type of control have been discussed, particularly when using fixed-point DSPs and relatively small computing power. To make it easy to implement resonance control using low-cost processors, the author proposed using phase-sensitive amplifiers and "all-pass" phase-shifter filters. Thus, using this technique, it is possible to implement the PR controller using 16-bit fixed-bit DSCs specifically developed for controlling power converters. In this chapter both the simulation and the analytical simulations were evaluated by the effects of the damping factor on the performance of the control (the occurrence of a stationary error that can be determined analytically and the modification of the system response to a "unit step" stimulus). The effects of the process of quantization and noise on the performance of the *PR* controller implemented in the z-domain were also evaluated.

In Chapter 4, the author evaluates the resonance control performance for the three major categories of variable-frequency converters: inverters, FAP and FP correction circuits. For each type of converter, parameters such as stationary error and current spectrum were evaluated using various control methods. In this chapter, the author proposes hybrid control for single-phase inverters. The hybrid control method involves running the resonance control in the s domain, and the generation of the reference signal as well as the PWM is done by a microcontroller in the z-domain. The primary objective of this method is to reduce the cost of the controller so that simple systems such as residential ones benefit from the benefits of this kind of control.

The practical results are presented in Chapter 5. The resonance control implementation methods proposed in Chapters 3 and 4 are evaluated using a hardware platform containing a single-phase inverter and a control and control board. The author implemented PR resonance control using the phase-based amplifier based method using a dsPIC33FJ16GS502 16-bit fixed-dot DSC. The measurements made confirm the feasibility of the proposed method; the implemented *PR* controller contains up to four resonant terms ensuring selective elimination of the third, fifth and seventh harmonics in the case of a non-linear load consisting of a single-phase rectifier followed by a capacitive filter and a resistor. Using the same control and control board, the operation and performance of the hybrid control were evaluated. And this method proves to be feasible and contributes to significant cost savings where this is important (in the case of micro-inverters found in *UPS*s).

6.2. Original Contributions

At the time of this thesis and following the author's knowledge, the following are original contributions:

- It is proposed to implement the resonant term that is part of the *PR* controller with two non-ideal integrators. This can simulate the effects introduced by the finite gain of the resonant term, which is encountered in a real implementation.
- A number of circuit topologies have been proposed and presented that can be used to implement the *PR* controller in the s-domain. These circuits can be used to simulate controllers controlled with *PR* controllers using simulators operating exclusively in the s domain or for implementing the hybrid control [O.8].
- The effects of the response time of the resonant term on the performance of the converter were analyzed. The effects of the final gain were also analyzed and the stationary error value introduced by this final gain.
- It was proposed to implement the resonant term using the phase-sensitive amplifier [O.7, O.8]. This makes it possible to implement *PR* control using low-cost fixed-float *DSP*s.
- It was proposed to use hybrid control for applications where the cost should be kept under control so now are micro-inverters [O.8]. In this case, the *PR* controller is

implemented in the s-domain while the reference signal generator as well as the PWM modulator are implemented in the z-domain using an 8-bit microcontroller.

- It was proposed to introduce a resonant term into the control loop of a *PFC* circuit [O.1]. This can improve performance especially for high power applications where the switching frequency is small, close to the reference signal frequency.

6.3 Original Papers

[O.1] Oprea S., Rădoi C., Florescu A., “Single-phase power factor correction circuit with Proportional-Resonant control”, ECAI 2014, October 23 – October 25, 2014.

[O.2] Oprea S., Hamzescu-Rosu M., Rădoi C., “Implementation of Simple MPPT Algorithms Using Low-Cost 8-Bit Microcontrollers”, ECAI 2014, October 23 – October 25, 2014.

[O.3] Florescu A., and Oprea S., "High Efficiency LLC resonant converter with digital control", Revue Roumaine des Sciences Techniques – Serie Electrotechnique et Energetique, pp. 183-192, ISSN 0035-4066, 2013.

[O.4] Adriana Florescu, Sergiu Oprea, "PV charger system using a synchronus buck converter", Proceedings of Simpozionul Naţional de Electrotehnică Teoretică (SNET 2013), 14 Decembrie 2012, Facultatea de Inginerie Electrică, Universitatea "Politehnica" din Bucureşti, pp. 238-243, ISSN 2067-4147

[O.5] Sergiu Oprea, Constantin Rădoi, Adriana Florescu, Andrei-Stefan Savu and Adrian-Ioan Lită, "Power Architectures and Power Conditioning Unit for Very Small Satellites", Lecture Notes in Energy vol. 37, Springer International Publishing AG 2017, ISBN 978-3-319-49874-4

[O.6] Andrei Cocor, Adriana Florescu, Ana-Maria Popescu, Dan-Alexandru Stoichescu, Sergiu Oprea „Power supply blocks with Cúk and self - lift Cúk converters for telecommunication sites”, International Symposium on Fundamentals of Electrical Engineering (ISFEE), 2014

[O.7] Mihnea Roșu-Hamzescu, Sergiu Oprea, Cristina Polonschii, Eugen Gheorghiu, Mihaela Gheorghiu, „High Performance Low Cost Impedance Spectrometer for Biosensing”, 21st International Conference on Control Systems and Computer Science, 2017

[O.8] S. Oprea, C. Rădoi, „On the implementation of resonant controllers in continuous and discrete time domains”, Scientific Bulletin of „Politehnica” University, Bucharest, 2018, in review for publication

6.4 Further Development

The topic addressed will continue to be topical as the interest in developing applications dedicated to the conversion of energy from alternative sources (solar panels, wind generators, etc.) remains high. With regard to further development, the following directions can be mentioned:

- Development of new methods for the implementation of resonant terms in the field of z that simultaneously ensure two goals: high precision, simplicity of theoretical analysis and practical achievement. This makes it possible to significantly reduce the time allocated to the controller calculations; so auxiliary tasks can be implemented by the processor such as spectral analysis of the error signal in the case of AFPs.

- The study of the implementation of resonant terms in the field using techniques such as the so-called "switched-capacitors filters". This ensures the high accuracy of the resonant frequency of the resonant term without the use of expensive and large components such as precision capacitors.

Selective Bibliography

[1] R. Bojoi, L. Limongi, F. Profumo, D. Roiu, and A. Tenconi, “Analysis of current controllers for active power filters using selective harmonic compensation schemes,” IEEJ Transactions on Electrical and Electronic Engineering, vol. 4, no. 2, pp. 139–157, 2009.
[2] S. Buso, L. Malesani, P. Mattavelli, “Comparison of current control techniques for active filter applications,” IEEE Transactions on Industrial Electronics, vol. 45, no. 5, pp. 722–729, Oct. 1998.
[3] S. Buso, S. Fasolo, L. Malesani, P. Mattavelli, “A dead-beat adaptive hysteresis current control,” IEEE Transactions on Industry Applications, vol. 36, no. 4, pp. 1174–1180, Jul. 2000.
[4] M. Kazmierkowski, L. Malesani, “Current control techniques for three-phase voltage source PWM converters: a survey,” IEEE Transactions on Industrial Electronics, vol. 45, no. 5, pp. 691–703, Oct. 1998.
[5] M. Kazmierkowski, L. Malesani, “Current control techniques for three-phase voltage source PWM converters: a survey,” IEEE Transactions on Industrial Electronics, vol. 45, no. 5, pp. 691–703, Oct. 1998.
[6] B. Bose, “An adaptive hysteresis-band current control technique of a voltage-fed PWM inverter for machine drive system,” IEEE Transactions on Industrial Electronics, vol. 37, no. 5, pp. 402–408, Oct. 1990
[7] M. Teodorescu, “Metode și Sisteme Avansate de Comandă pentru Filtre Active de Putere”, Teza de doctorat, 2012
[8] P. Mattavelli, “An improved deadbeat control for UPS using disturbance observers,” IEEE Transactions on Industrial Electronics, vol. 52, no. 1, pp. 206–212, Feb. 2005
[9] P. Chapman, S. Sudhoff, “A multiple reference frame synchronous estimator/ regulator,” IEEE Transactions on Energy Conversion, vol. 15, no. 2, pp. 197–202, Jun. 2000.
[10] P. Mattavelli, “A closed-loop selective harmonic compensation for active filters,” IEEE Transactions on Industry Applications, vol. 37, no. 1, pp. 81–89, Jan./Feb. 2001.
[11] M. Tomizuka, "Zero phase error tracking algorithm for digital control", J. OD Dynamic Systems Measurements Control, vol. 109, pp. 65-68, Mar. 1987.
[12] R. I. Bojoi, G. Griva, V. Bostan, M. Guerriero, F. Farina, and F. Profumo, “Current control strategy for power conditioners using sinusoidal signal integrators in synchronous reference frame,” IEEE Transactions on Power Electronics, vol. 20, no. 6, pp. 1402– 1412, Nov. 2005.
[13] D. Roiu, R. I. Bojoi, L. R. Limongi, and A. Tenconi, “New stationary frame control scheme for three-phase PWM rectifiers under unbalanced voltage dips conditions,” IEEE Transactions on Industry Applications, vol. 46, no. 1, pp. 268–277, Jan./Feb. 2010.
[14] R. Teodorescu, F. Blaabjerg, M. Liserre, and P. C. Loh, “Proportional-resonant controllers and filters for grid-connected voltage-source converters,” in IEE Proceedings - Electric Power Applications, vol. 153, no. 5, Sep. 2006, pp. 750–762.
[15] R. Teodorescu, F. Blaabjerg, U. Borup, and M. Liserre, “A new control structure for grid-connected LCL PV inverters with zero steady-state error and selective harmonic compensation,” in Proceedings of IEEE Applied Power Electronics Conference, APEC, vol. 1, 2004, pp. 580–586
[16] R. Teodorescu, F. Blaabjerg, M. Liserre, P.C. Loh, “Proportional-resonant controllers and filters for grid-connected voltage-source converters,” IEE Proc.-Electr. Power Appl., Vol. 153, No. 5, Sep. 2006

[17] R. Teodorescu, F. Blaabjerg, M. Liserre, “Proportional-Resonant Controllers. A New Breed of Controllers Suitable for Grid-Connected Voltage-Source Converters,’ Journal of Electrical Engineering, 2006
[18] M. Newman, D. Holmes, J. Nielsen, F. Blaabjerg, “A dynamic voltage restorer (DVR) with selective harmonic compensation at medium voltage level,” IEEE Transactions on Industry Applications, vol. 41, no. 6, pp. 1744–1753, Nov./Dec. 2005.
[19] A. V. Timbus, M. Ciobotaru, R. Teodorescu, F. Blaabjerg, “Adaptive resonant controller for grid-connected converters in distributed power generation systems,” in Proceedings of IEEE Applied Power Electronics Conference, APEC, Mar. 2006.
[20] A. G. Yepes, F. D. Freijedo, J. Doval-Gandoy, O. Lopez, J. Malvar, P. Fernandez-Comesana, “Effects of Discretization Methods on the Performance of Resonant Controllers,” IEEE Transactions on Power Electronics, vol. 25, no. 7, July 2010
[21] A. G. Yepes, Francisco D. Freijedo, Oscar Lopez, Jesus Doval-Gandoy, “High-Performance Digital Resonant Controllers Implemented With Two Integrators,” IEEE Transactions on Power Electronics, vol. 26, no. 2, Feb. 2011
[22] A. G. Place, G. H. Allen, “Generalized Pole Sensitivity Analysis Due to Parameter Perturbation,” IEEE Transactions on Circuits and Systems—II: Analog and Digital Signal Processing, vol. 44, no. 10, October 1997
[23] A. G. Place, G. H. Allen, “Perturbation Effects on Filters Having Localized Poles,” International Conference on Acoustics, Speech, and Signal Processing, May 1995
[24] Phillip A. Regalia, Sanjit K. Mitra, P. P. Vaidyanathan “The Digital All-Pass Filter: A Versatile Signal Processing Building Block,” Proceedings of the IEEE, Vol. 76, No. 1, Jan. 1988
[25] B. Widrow, “Statistical Analysis of Amplitude-Quantized Sampled-Data Systems, “Transactions of the American Institute of Electrical Engineers, Part II: Applications and Industry, Vol. 79, Issue 6, Jan. 1961
[26] G. Chiorboli, “Uncertainty of Mean Value and Variance Obtained from Quantized Data,” IEEE Instrumentation and Measurement Technology Conference Anchorage, Alaska, USA, 21-23 May, 2002
[27] M. F. Wagdy, W-M Ng, “Validity of Uniform Quantization Error Model for Sinusoidal Signals Without and With Dither,” IEEE Transactions on Instrumentation and Measurement. vol. 38. no. 3. June 1989
[28] S. Buso, P. Mattavelli, Digital Control in Power Electronics. J. Hudgins, Ed. Morgan and Claypool Publishers, 2006.
[29] G. C. Goodwin, S. F. Graebe, M. E. Salgado, Control System Design. Prentice Hall, 2000.
[30] H. T. N. Charles L. Phillips, Digital Control System Analysis and Design,. 3rd Edition. Prentice Hall, 1995.
[31] R. Teodorescu, M. Liserre, P. Rodríguez, Grid Converters for Photovoltaic and Wind Power Systems. 1st ed. Wiley-IEEE Press, 2011.
[32] K. Ogata, Modern Control Engineering. Prentice Hall, 2009.
[33] M. Kazmierkowski, R.Krishnan, F.Blaabjerg, Control in Power Electronics. Selected Problems, Academic Press 2002, ISBN 0-12-402772-5.
[34] Jean-J. E. Slotine, W. Li, Applied Nonlinear Control. Prentice Hall, 1991
[35] R. W. Erickson, D. Maksimovic, Fundamentals of Power Electronics, 2nd ed., New York, Kluwer Academic Publishers, 2004.